The Canadian Mineralogist
Vol. 41, pp. 1481-1501 (2003)

CRYSTAL STRUCTURES AND CRYSTAL CHEMISTRY OF MEMBERS OF THE CUPROBISMUTITE HOMOLOGOUS SERIES OF SULFOSALTS

DAN TOPA[§]

Geological Institute, University of Salzburg, Hellbrunnerstr. 34/III, A–5020 Salzburg, Austria

EMIL MAKOVICKY[§] AND TONČI BALIĆ-ŽUNIĆ[§]

Geological Institute, University of Copenhagen, Østervoldgade 10, DK–1350 Copenhagen K, Denmark

ABSTRACT

Crystal structures of natural cuprobismutite, $Cu_{8.05}$ $(Bi_{12.83}Ag_{0.96}Pb_{0.15}Cd_{0.08})_{\Sigma 14.02}$ $S_{23.93}$, from Felbertal, Austria, with *a* 17.590(4), *b* 3.922(1), *c* 15.177(3) Å, β 100.710(4)°, space group *C*2/*m*, *Z* = 1, and of two samples of hodrushite: (1) $(Cu_{7.48}Fe_{0.45})_{\Sigma 7.93}$ $(Bi_{11.54}Ag_{0.40}Pb_{0.08})_{\Sigma 12.02}$ $S_{22.05}$, also from Felbertal, with *a* 17.562(1), *b* 3.920(1), *c* 27.150(2) Å, β 92.561(1)°, space group *C*2/*m*, *Z* = 2, and (2) $(Cu_{8.08}Fe_{0.28})_{\Sigma 8.36}$ $(Bi_{11.51}Ag_{0.03}Pb_{0.08}Sb_{0.03}Cd_{0.08})_{\Sigma 11.73}$ $S_{21.91}$, from Swartberg, South Africa, with *a* 17.535(4), *b* 3.900(1), *c* 27.109(4) Å, β 92.333(9)°, space group *C*2/*m*, *Z* = 2, were refined from single-crystal X-ray data. Eight samples of cuprobismutite homologues were analyzed with an electron microprobe. All homologues consist of PbS-like accretional (a) slabs of two distinct thicknesses (kupčíkite-like *N* = 1 slabs and cuprobismutite-like *N* = 2 slabs) interleaved with (b) slabs combining paired coordination pyramids of Bi with Cu tetrahedra. Bismuth occurs in four distinct types of coordination polyhedra, from regular octahedra to capped prismatic polyhedra; copper occurs in trigonal planar and tetrahedral coordination. Silver substitutes for Bi in the central octahedron of cuprobismutite-like slabs, and Pb possibly as well, whereas Fe^{3+} substitutes for Cu along the boundaries of kupčíkite-like slabs. In the hodrushite from Swartberg, Cu substitutes for octahedrally coordinated Bi, as is the case in synthetic cuprobismutite. Multiple correlations among substitution trends were observed.

Keywords: cuprobismutite, hodrushite, kupčíkite, single-crystal X-ray diffraction, electron-microprobe data, cuprobismutite homologous series, substitution trends, crystal chemistry.

SOMMAIRE

Les structures cristallines de la cuprobismutite naturelle, $Cu_{8.05}$ $(Bi_{12.83}Ag_{0.96}Pb_{0.15}Cd_{0.08})_{\Sigma 14.02}$ $S_{23.93}$, provenant de Felbertal, en Autriche, *a* 17.590(4), *b* 3.922(1), *c* 15.177(3) Å, β 100.710(4)°, groupe spatial *C*2/*m*, *Z* = 1, et de deux échantillons de hodrushite: (1) $(Cu_{7.48}Fe_{0.45})_{\Sigma 7.93}$ $(Bi_{11.54}Ag_{0.40}Pb_{0.08})_{\Sigma 12.02}$ $S_{22.05}$, aussi de Felbertal, *a* 17.562(1), *b* 3.920(1), *c* 27.150(2) Å, β 92.561(1)°, groupe spatial *C*2/*m*, *Z* = 2, et (2) $(Cu_{8.08}Fe_{0.28})_{\Sigma 8.36}$ $(Bi_{11.51}Ag_{0.03}Pb_{0.08}Sb_{0.03}Cd_{0.08})_{\Sigma 11.73}$ $S_{21.91}$, provenant de Swartberg, en Afrique du Sud, *a* 17.535(4), *b* 3.900(1), *c* 27.109(4) Å, β 92.333(9)°, groupe spatial *C*2/*m*, *Z* = 2, ont été affinées à partir de données en diffraction X prélevées sur monocristal. Huit échantillons d'homologues de la cuprobismutite ont été analysés avec une microsonde électronique. Tous les homologues sont faits de panneaux accrétionnels de type PbS (a) de deux épaisseurs différentes (de type kupčíkite, *N* = 1, et de type cuprobismutite, *N* = 2) interstratifiés avec des panneaux (b) contenant des pyramides de tétraèdres à Bi et Cu en paires. Le bismuth se présente en quatres types de polyèdre de coordinence, variant d'octaèdre régulier à polyèdre prismatique chapeauté; le cuivre se présente en coordinence trigonale en plan et en coordinence tétraédrique. L'argent remplace le Bi dans l'octaèdre central des panneaux de type cuprobismutite, et même le Pb, tandis que le Fe^{3+} remplace le Cu le long des bordures des panneaux de type kupčíkite. Dans la hodrushite de Swartberg, le Cu remplace le Bi en coordinence octaédrique, tout comme dans la cuprobismutite synthétique. De multiples corrélations parmi les vecteurs de substitution sont présentes.

(Traduit par la Rédaction)

Mots-clés: cuprobismutite, hodrushite, kupčíkite, diffraction X sur monocristal, données de mirosonde électronique, série des homologues de la cuprobismutite, vecteurs de substitution, cristallochimie.

§ *E-mail addresses*: dan.topa@sbg.ac.at, emilm@geo.geol.ku.dk, tonci@geo.geol.ku.dk

Introduction

Cuprobismutite, hodrushite, and kupčíkite are the three known members of the cuprobismutite homologous series of Cu–Bi sulfosalts (Makovicky 1989). Cuprobismutite was described by Hillebrand (1884) as an unnamed mineral of ideal composition $3(Cu,Ag)_2S•4Bi_2S_3$. Dana (1892) assigned it the current name. Nuffield (1952) obtained a monoclinic unit-cell with *a* 17.65, *b* 3.93, and *c* 15.24 Å, β 100.5°, space group *C*2/*m* from the type material. He managed to synthesize silver-free cuprobismutite, tentatively assigned it a formula $CuBiS_2$, and considered it dimorphous with emplectite. The crystal structure of synthetic cuprobismutite was determined by Ozawa & Nowacki (1975); these authors found a composition of $Cu_{10.4}Bi_{12.6}S_{24}$, with some Bi sites largely filled by Cu.

Hodrushite was described by Koděra *et al.* (1970); electron-microprobe data were reported by Makovicky & MacLean (1972), and the structure determination, by Kupčik & Makovicky (1968). Its composition was quoted as $Cu_{8.12}Bi_{11.54}Fe_{0.29}S_{22}$, with unspecified, small amounts of Pb. The unit cell, *a* 27.21, *b* 3.94, and *c* 17.58 Å, β 92.9°, space group *A*2/*m*, indicated its relationship to cuprobismutite. This relationship was defined in Koděra *et al.* (1970) by reference to the results of Kupčik & Makovicky (1968): the structure of hodrushite is a regular intergrowth of cuprobismutite-like slabs with slabs of a hitherto undescribed Cu–Bi sulfosalt. This relationship was confirmed and refined by Mariolacos *et al.* (1975), who synthesized the "missing slab" as an independent phase. Its composition was given by them as $Cu_4Bi_5S_{10}$ with *a* 17.54, *b* 3.93, *c* 12.85 Å, β 108°, space group *C2/m*. Nobody else managed to synthesize this phase, but Sugaki *et al.* (1981) synthesized "phase Z", to which they assigned the composition $Cu_{8.4}Fe_{1.2}Bi_{10.8}S_{22}$, analogous to hodrushite, although its unit-cell parameters are practically identical to those of $Cu_4Bi_5S_{10}$. Topa *et al.* (2003) described the natural occurrence of such a phase, $Cu_{3.4}Fe_{0.6}Bi_5S_{10}$, as kupčíkite, and determined its structure.

Two structure types are related to the cuprobismutite homologous series, synthetic $Cu_4Bi_4S_9$ (Takéuchi & Ozawa 1975, Bente & Kupčik 1984) and the isostructural $Cu_4Bi_4Se_9$ (Makovicky *et al*. 2002) on the one hand, and paderaite $Ag_{1.2}Cu_{5.8}Pb_{1.3}Bi_{11.5}S_{22}$ (Mumme 1986) on the other. Both of them share many features with cuprobismutite homologues, but differ from them in several substantial "non-homologous" features; they are "plesiotypic" with respect to this homologous series (Makovicky 1997).

All three members of the cuprobismutite homologous series contain minor elements, Ag, Fe and Pb, in variable amounts. For some of them, the presence of Cu-for-Bi substitution was inferred from electron-microprobe data, as was observed by Ozawa & Nowacki (1975). Makovicky (1989) stated that "among the members of an accretional series, the composition changes regularly and by increments; therefore the electron-microprobe data for the microscopic grains of such phases can be used to evaluate the order number of the homologue." Unfortunately, such a procedure is in principle not applicable to the cuprobismutite homologues because of the unknown extent of the Cu-for-Bi substitution and its influence on stoichiometry. Moreover, assignments of minor elements to Cu or Bi sites has remained problematic.

In present paper, we seek to amend this situation by means of determinations of the exact structure of preanalyzed crystals from well-characterized samples. The present determinations of the structures (including that on kupčíkite by Topa *et al.* 2003) not only confirm the structural schemes for individual members of the series, but also allow an assessment of the extent of the Cu-for-Bi substitution in the natural homologues as well as an assignment of minor elements to individual structural sites. This approach leads to a revised structural formula for the entire series which, with the exception of samples with extensive Cu-for-Bi substitution (rare in nature), automatically leads to a correct assignment of the homologue order number *N* (*i.e.*, mineral determination) from results of the chemical analysis alone.

We do not attempt to collect literature data on potential cuprobismutite homologues and re-evaluate them. This exercise requires a time-related re-assessment of the reliability of all the electron-microprobe data accumulated since about 1968 (*cf.* problems with the ZAF correction cited by Makovicky & MacLean 1972), among other factors, and is relegated to other publications.

Provenance of the Samples

Electron-microprobe analyses were performed on samples from five localities: Felbertal (Austria), Hodrusha (Slovakia), Swartberg (South Africa), as well as Băiţa Bihor and Ocna de Fier (Romania). As part of this project, crystal structures were determined for cuprobismutite (Felbertal), hodrushite (Felbertal and Swartberg), for comparison with results on kupčíkite from Felbertal (Topa *et al.* 2003).

In the Felbertal scheelite deposit, Hohe Tauern, Austria, cuprobismutite homologues are known only in the orebodies K7 and K8 (Topa 2001, Topa *et al.* 2002, 2003). These orebodies lie in amphibolite with lenses of leucocratic gneisses and quartz masses. The ore is believed to be related to Variscan magmatic events and was reworked during Alpine metamorphism.

Cuprobismutite homologues occur associated with makovickyite (pavonite homologue ^{4}P), cupromakovickyite (modified ^{4}P) and bismuthinite derivatives, with 50–96 mol.% of the aikinite end-member. Simple and multiple parallel intergrowths of kupčíkite–hodrushite (Topa *et al.* 2003, Fig. 5) and hodrushite–cuprobismutite (Figs. 1a, b) display sharp, straight boundaries between the intergrown components. The

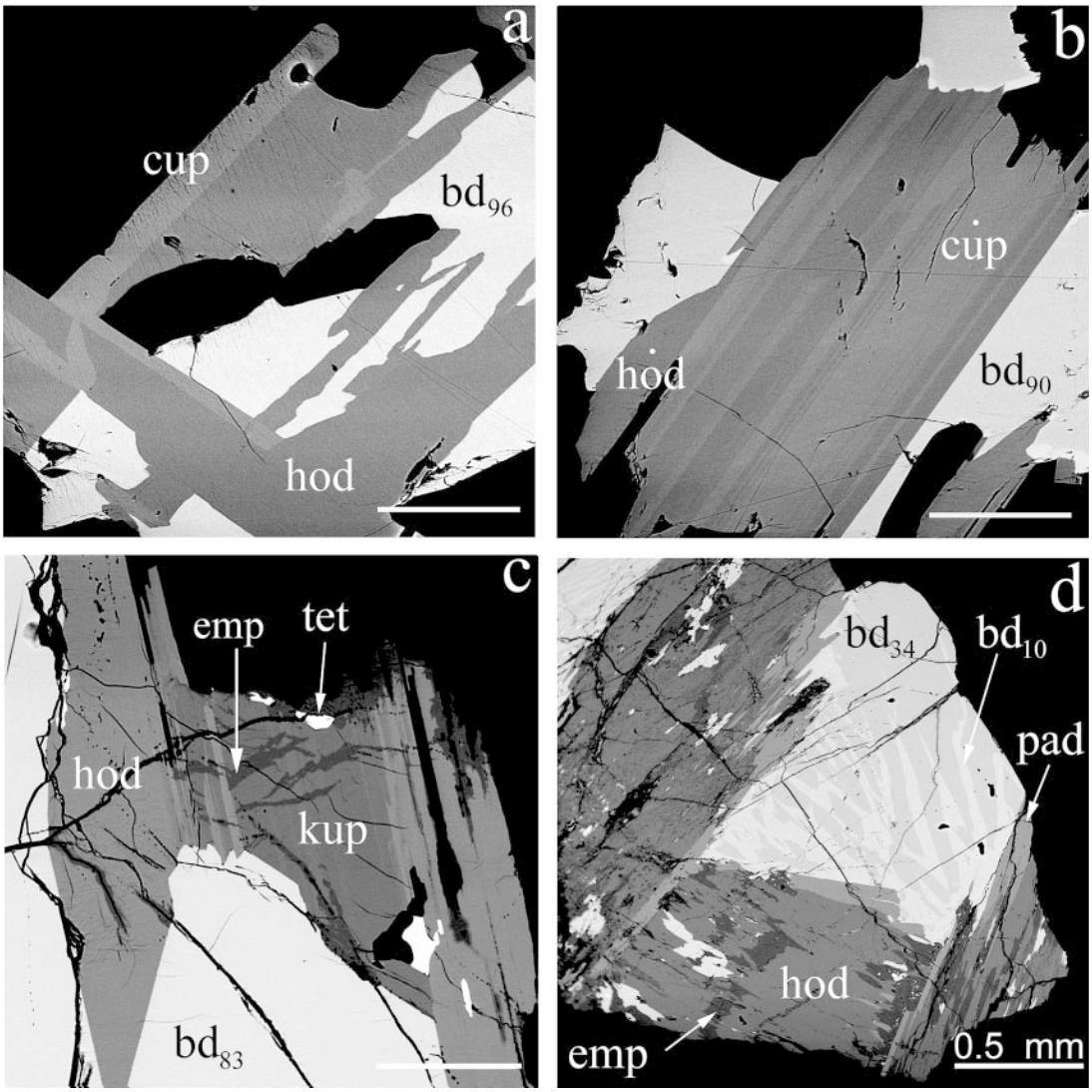

FIG. 1. Typical aggregates of cuprobismutite homologues and associated phases from: a) and b) Felbertal, K8 ore body, Austria, c) Băiţa Bihor, Romania, and d) Swartberg, South Africa. Where not indicated, bar length is 100 μm. Abbreviations: cup: cuprobismutite, kup: kupčíkite, hod: hodrushite, emp: emplectite, pad: paděraite, tet: tetradymite, bd_{xx}: bismuthinite derivative, with the percentage of the aikinite end-member indicated.

association kupčíkite–cuprobismutite is characterized by the replacement of the latter by the former. Native Bi is a late product of decomposition.

The Cu–(Ag)–Pb–Bi sulfosalt assemblages from Triassic skarn deposits at Băiţa Bihor, Apuseni Mountains, Romania (Cioflica & Vlad 1973, Žák *et al.* 1994) consist of bismuthinite derivatives with 50–89 mol.% of the aikinite end-member, makovickyite, cupromakovickyite, hodrushite, kupčíkite, paděraite and tetradymite. The specimen studied contains a parallel intergrowth of hodrushite and kupčíkite with indistinct signs of a replacement texture, and with emplectite as the final product (Fig. 1c). A bismuthinite derivative with 83 mol.% of aikinite end-member replaces both phases; grains of tetradymite are scattered in the aggregates.

In the sample from Swartberg, South Africa (Ciobanu & Cook 2002), composite crystals of hodrushite are lined by splintery crystals of paděraite,

probably an older phase. The intermediate spaces are filled by a bismuthinite derivative decomposed into a coarse intergrowth of a derivative with 10 mol.% and a derivative with 34 mol.% of aikinite end-member. Emplectite replaces primarily hodrushite and paděraite (Fig. 1d). A description of the Swartberg occurrence as well as the Ocna de Fier deposit will be given by Cook *et al.* (in prep.).

Experimental

Chemical analysis

Quantitative chemical analyses were performed with a JEOL JXA–8600 electron microprobe controlled by a LINK–*eXL* system, operated at 25 kV, and 30 nA, with 20 s counting time for peaks and 7 s for background. The following natural (n) and synthetic (s) standards and X-ray lines were used: n-$CuFeS_2$ (Cu$K\alpha$, Fe$K\alpha$), s-Bi_2S_3 (Bi$L\alpha$, S$K\alpha$), n-PbS (Pb$L\alpha$), s-CdTe (Cd$L\beta$, Te$L\alpha$), n-Sb_2S_3 (Sb$L\alpha$) and pure metal for Ag$L\alpha$. Raw data were corrected with the on-line ZAF–4 procedure. Standard deviations (error in wt.%) of elements sought for the cuprobismutite series are: Bi 0.17, Pb, Cd and S 0.06, Cu 0.04, Ag 0.03, Sb 0.02 and Fe 0.01. Results of three to five point-analyses obtained from a homogeneous grain or an individual phase in an aggregate were averaged. Chemical data for the material structurally investigated, as well as for mineral assemblages presented in Figure 1, are compiled in Table 1.

Single-crystal X-ray diffraction

Fragments of cuprobismutite with an irregular shape and a diameter of 0.03–0.07 mm from Felbertal and fragments of hodrushite from Felbertal and Swartberg were measured on a Bruker AXS four-circle diffractometer equipped with a CCD area detector using graphite monochromated Mo$K\alpha$ radiation. Crystal data for the grains studied are listed in Table 2. The SMART

TABLE 1. CHEMICAL COMPOSITION OF THE MEMBERS OF THE CUPROBISMUTITE HOMOLOGOUS SERIES

No.	Phase	SAMPLE	Fig.	#	Cu	Ag	Fe	Pb	Cd	Bi	Sb	S	Total	N_{chem}	cb	ev	Σmet	*Na*
1*	kupčíkite	FE-89/9-sg29-d		5	13.02	0.11	2.23	0.00	0.30	64.21	0.12	20.10	100.08	1.05	0.07	0.17	17.87	38
2*	hodrushite	FE-89/9-sg6am		5	12.93	1.19	0.68	0.42	0.00	65.54	0.00	19.22	99.99	1.53	-0.11	-0.25	19.95	42
3*	cuprobismutite	FE-89/9-1-18m		5	12.50	2.54	0.00	0.75	0.22	65.48	0.00	18.74	100.23	1.98	0.12	0.25	22.08	46
4*	hodrushite	Swartberg		5	14.02	0.10	0.42	0.43	0.24	65.71	0.08	19.21	100.22	1.31	0.00	0.00	20.08	42
5	cuprobismutite	Ocna de Fier		5	12.39	2.47	0.00	0.86	0.19	65.53	0.00	18.70	100.14	2.01	0.15	0.31	22.06	46
6	hodrushite	Hodrusha		5	13.37	1.26	0.47	0.44	0.17	65.39	0.00	19.10	100.22	1.50	0.08	0.18	20.11	42
7	cuprobismutite	Fe-89/9-4-g24	1a	5	12.20	2.52	0.00	1.27	0.00	65.62	0.00	18.74	100.35	2.08	0.02	0.04	21.99	46
8	hodrushite	Fe-89/9-4-g24	1a	5	13.15	0.90	0.48	0.29	0.00	65.47	0.00	18.98	99.26	1.50	-0.02	-0.05	20.00	42
9	cuprobismutite	Fe-89/9-4-30	1b	5	12.39	2.50	0.00	0.81	0.27	65.06	0.00	18.70	99.72	1.99	-0.06	-0.13	22.03	46
10	hodrushite	Fe-89/9-4-g30	1b	5	13.18	1.08	0.51	0.30	0.00	65.42	0.00	19.06	99.54	1.50	-0.07	-0.16	20.01	42
11	kupčíkite	Băiţa Bihor	1c	5	13.78	0.00	1.55	0.00	0.31	64.87	0.20	19.90	100.62	1.07	0.02	0.05	18.02	38
12	hodrushite	Băiţa Bihor	1c	5	13.13	1.11	0.58	0.48	0.21	65.27	0.14	19.15	100.08	1.52	0.08	0.18	20.04	42
13	hodrushite	Swartberg	1d	5	13.81	0.09	0.44	0.40	0.22	65.31	0.15	19.18	99.59	1.33	-0.20	-0.45	20.00	42
14	paděraite	Swartberg	1d	5	12.06	0.00	0.00	7.29	0.00	61.34	0.09	18.33	99.11		-0.01	-0.02	19.99	44

The raw data are quoted in wt.%. * Grains used for single-crystal structural investigations; #: number of analyses. FE: sample from Felbertal, N_{chem}: chemical number of the homologue, cb: charge balance (with Fe^{3+}), ev: error relative to the total of valences, *Na*: number of atoms per formula unit. The formulae are based on the following total values of *Na*: 38 for kupčikite, 42 for cuprobismutite, 46 for hodrushite and 44 for paděraite.

1) $(Cu_{6.58}Fe_{1.28})_{\Sigma 7.86}\,(Bi_{9.87}Ag_{0.03}Sb_{0.03}Cd_{0.09})_{\Sigma 10.02}\,S_{20.13}$
2) $(Cu_{7.48}Fe_{0.45})_{\Sigma 7.93}\,(Bi_{11.54}Ag_{0.40}Pb_{0.08})_{\Sigma 10.02}\,S_{22.05}$
3) $Cu_{8.05}\,(Bi_{12.83}Ag_{0.96}Pb_{0.15}Cd_{0.08})_{\Sigma 14.02}\,S_{23.93}$
4) $(Cu_{7.72}Fe_{0.28})_{\Sigma 8.00}\,Cu_{0.36}\,(Bi_{11.51}Ag_{0.03}Sb_{0.03}Pb_{0.08}Cd_{0.08})_{\Sigma 11.73}\,S_{21.91}$
5) $Cu_{8.00}\,(Bi_{12.87}Ag_{0.94}Pb_{0.17}Cd_{0.07})_{\Sigma 14.05}\,S_{23.95}$
6) $(Cu_{7.73}Fe_{0.31})_{\Sigma 8.04}\,(Bi_{11.50}Ag_{0.43}Sb_{0.03}Pb_{0.00}Cd_{0.09})_{\Sigma 12.07}\,S_{21.89}$
7) $Cu_{7.88}\,(Bi_{12.90}Ag_{0.96}Pb_{0.25})_{\Sigma 14.11}\,S_{24.01}$
8) $(Cu_{7.69}Fe_{0.31})_{\Sigma 8.00}\,(Bi_{11.64}Ag_{0.31}Pb_{0.05})_{\Sigma 12.00}\,S_{22.00}$
9) $Cu_{8.02}\,(Bi_{12.80}Ag_{0.95}Pb_{0.16}Cd_{0.10})_{\Sigma 14.01}\,S_{23.97}$
10) $(Cu_{7.67}Fe_{0.34})_{\Sigma 8.01}\,(Bi_{11.58}Ag_{0.37}Pb_{0.05})_{\Sigma 12.00}\,S_{21.99}$
11) $(Cu_{6.98}Fe_{0.89})_{\Sigma 7.87}\,(Bi_{10.00}Sb_{0.05}Cd_{0.07})_{\Sigma 10.12}\,S_{20.01}$
12) $(Cu_{7.75}Fe_{0.32})_{\Sigma 8.07}\,(Bi_{11.51}Ag_{0.29}Sb_{0.05}Pb_{0.08}Cd_{0.07})_{\Sigma 12.00}\,S_{21.93}$
13) $(Cu_{7.71}Fe_{0.29})_{\Sigma 8.00}\,Cu_{0.29}\,(Bi_{11.50}Ag_{0.03}Sb_{0.05}Pb_{0.07}Cd_{0.06})_{\Sigma 11.71}\,S_{22.00}$
14) $Cu_{7.31}\,(Bi_{11.30}Sb_{0.03}Pb_{1.36})_{\Sigma 12.69}\,S_{22.01}$; phase related to the cuprobismutite series.

TABLE 2. SINGLE-CRYSTAL X-RAY-DIFFRACTION OF CUPROBISMUTITE AND HODRUSHITE: EXPERIMENTAL AND REFINEMENT DETAILS

Crystal data	cuprobismutite (Felbertal)	hodrushite (Felbertal)	hodrushite (Swartberg)
Chemical formula	$Cu_{8.05}Ag_{0.96}Bi_{13.06}S_{23.93}$	$Cu_{7.48}Fe_{0.45}Ag_{0.40}Bi_{11.62}S_{22.05}$	$Cu_{8.08}Fe_{0.28}Bi_{11.73}S_{21.91}$
Chemical formula weight	4104.35	7353.69	7344.37
Cell setting	Monoclinic	Monoclinic	Monoclinic
Space group	*C2/m*	*C2/m*	*C2/m*
a (Å)	17.590(4)	17.562(1)	17.527(3)
b (Å)	3.9219(7)	3.9201(3)	3.901(6)
c (Å)	15.177(3)	27.150(2)	27.120(4)
β (°)	100.710(4)	92.561(1)	92.343(7)
V (Å^3)	1028.8(6)	1867.3(4)	1852.9(6)
Z	1	2	2
D_x (g/cm^3)	6.625	6.539	6.582
No. of reflections for cell parameters	699	3461	1015
μ (mm^{-1})	61.12	60.23	61.02
Crystal form	irregular	irregular	irregular
Crystal size (mm)	0.03 × 0.03 × 0.04	0.03 × 0.035 × 0.07	0.02 × 0.045 × 0.07
Crystal color	black	black	black
Data collection			
T_{min}	0.011	0.004	0.071
T_{max}	0.034	0.019	0.163
No. of meas. reflections	5330	8888	10916
No. of ind. reflections	1730	3197	3134
No. of obs. reflections	1325	2490	2669
Criterion for observed reflections: $I > 2\sigma(I)$			
R_{int}	10.09%	5.41%	6.48%
θ_{max}(°)	30.66	30.53	36.55
Range of *h, k, l*	$-24 < h < 24$ $-5 < k < 5$ $-21 < l < 21$	$-24 < h < 23$ $-5 < k < 5$ $-38 < l < 38$	$-25 < h < 25$ $-4 < k < 5$ $-38 < l < 36$
Refinement			
Refinement on F_o^2			
$R[F_o > 4\sigma(F_o)]$	6.18%	4.25%	5.21%
$wR(F_o^2)$	15.95%	10.66%	14.01%
S (*GooF*)	1.007	0.975	1.070
No. of reflections used in refinement	1325	3197	3134
No. of parameters refined	72	63	133
Weighting scheme	(1)	(2)	(3)
$(\Delta/\sigma)_{max}$	0.003	0.001	0.002
$\Delta\rho_{max}$ (*e*/Å^3)	10.18 (1.26 Å from Cu1)	3.15 (0.81 Å from Bi1)	5.587 (0.56 Å from Cu1B)
$\Delta\rho_{min}$ (*e*/Å^3)	–3.74 (1.15 Å from Bi2)	–4.46 (0.03 Å from Bi5)	–5.079 (0.82 Å from *Me*1)
Extinction method		none	
Source of atomic scattering factors:	*International Tables for Crystallography* (1992, Vol. C, Tables 4.2.6.8 and 6.1.1.4)		
Computer programs			
Structure solution	*SHELXS97* (Sheldrick 1990)		
Structure refinement	*SHELXL97* (Sheldrick 1997)		

Weighing schemes: (1): $w = 1/[\sigma^2(F_o^2) + (0.0958P)^2]$; (2) $w = 1/[\sigma^2(F_o^2) + (0.0639P)^2]$, where $P = (F_o^2 + 2F_c^2)/3$; (3) $w = 1/[\sigma^2(F_o^2) + (0.0853P)^2]$.

(Bruker AXS, 1998) system of programs was used for unit-cell determination and data collection, SAINT+ (Bruker AXS, 1998) for the calculation of integrated intensities, and XPREP (Bruker AXS, 1998) for empirical absorption correction based on pseudo Ψ-scans. The centrosymmetric space-group *C2/m*, proposed by the XPREP program, was chosen and is consistent with the monoclinic symmetry of the lattices and intensity statistics. The structures were solved by direct methods (program SHELXS, Sheldrick 1997a) that revealed most of the cation positions. In subsequent cycles of the refinement (program SHELXL, Sheldrick 1997b), cation positions were deduced from difference-Fourier syntheses by selecting from among the strongest maxima at appropriate distances. Thus, the new structure solutions were independent of the published results. As can be seen in Table 1, the results of the structure refinement for cuprobismutite do not match those on the hodrushite and kupčíkite samples. Even the best fragment of cuprobismutite available displays a slightly domain-like texture with spurious amounts of other sulfides intergrown (bismuthinite derivative).

Results of the refinement are given in Table 2, fractional coordinates, isotropic and anisotropic displacement parameters of the atoms are listed in Tables 3a–c, and selected *Me*–S bond distances are presented in Table 4. Selected geometrical parameters, calculated with IVTON program (Balić-Žunić & Vicković 1996), related to individual coordination polyhedra are given in Table 5. The structures of cuprobismutite homologues are presented in Figures 2–5, which show the site labeling for cuprobismutite and hodrushite structures. Tables

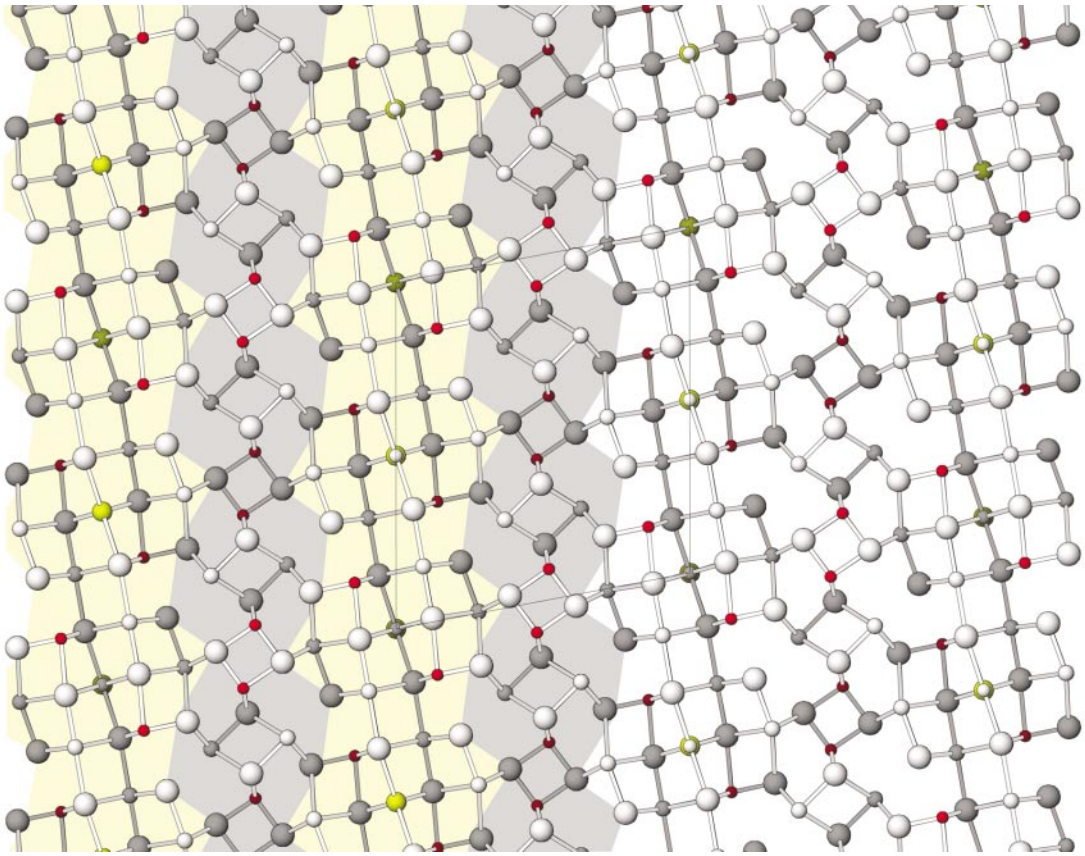

FIG. 2. The crystal structure of cuprobismutite $Cu_{8.05}$ $(Bi_{12.83}Ag_{0.96}Pb_{0.15}Cd_{0.08})_{\Sigma 14.02}$ $S_{23.93}$ from Felbertal. Projection along [010], *a* axis 17.59 Å, *c* axis 15.177 Å. Shaded and void circles indicate two levels of *y*, approximately 2 Å apart. Bi1 represents a mixed Ag (yellow), Bi (grey) position. Two thin layers (grey-shaded) and two cuprobismutite-like layers (yellow-shaded), are indicated.

TABLE 3a. SITE LABELS, OCCUPANCY FACTORS, FRACTIONAL ATOMIC COORDINATES, EQUIVALENT ISOTROPIC AND ANISOTROPIC DISPLACEMENT PARAMETERS FOR CUPROBISMUTITE

site[a]	sof	*x/a*	*y/b*	*z/c*	U_{iso}	U_{11}	U_{22}	U_{33}	U_{13}
Bi1	0.292(8)	0.0	0.5	0.0	0.0304(6)	0.0280(9)	0.0295(11)	0.0341(11)	0.0068(7)
Ag1	0.708(8)	0.0	0.5	0.0	0.0304(6)	0.0280(9)	0.0295(11)	0.0342(11)	0.0068(7)
Bi2		0.33456(4)	0.5	0.09272(5)	0.0293(2)	0.0300(4)	0.0219(4)	0.0340(5)	0.0012(3)
Bi3		0.49537(5)	0.0	0.28002(6)	0.0293(2)	0.0311(4)	0.0239(4)	0.0321(4)	0.0038(3)
Bi4		0.24520(4)	0.5	0.37071(5)	0.0270(2)	0.0250(4)	0.0248(4)	0.0307(4)	0.0037(3)
Cu1		0.15528(29)	0.0	0.14082(24)	0.0562(10)	0.0929(31)	0.0416(20)	0.0360(17)	0.0166(19)
Cu2		0.08802(18)	0.0	0.47966(23)	0.0399(7)	0.0348(15)	0.0365(17)	0.0478(17)	0.0060(13)
S1		0.16381(33)	0.5	0.05920(36)	0.0294(11)	0.0353(27)	0.0230(26)	0.0287(25)	0.0027(20)
S2		0.48973(29)	0.5	0.12471(37)	0.0275(10)	0.0252(23)	0.0267(26)	0.0311(24)	0.0066(17)
S3		0.34252(28)	0.0	0.22009(35)	0.0255(10)	0.0215(21)	0.0232(25)	0.0315(25)	0.0046(17)
S4		0.15341(27)	0.0	0.28959(34)	0.0253(10)	0.0203(21)	0.0232(24)	0.0315(24)	0.0028(17)
S5		0.46745(31)	0.5	0.38695(35)	0.0277(10)	0.0309(24)	0.0238(25)	0.0294(25)	0.0082(19)
S6		0.16142(31)	0.5	0.49378(35)	0.0265(10)	0.0285(23)	0.0206(24)	0.0288(23)	0.0017(18)

of structure factors may be obtained from the Depository of Unpublished Data, CISTI, National Research Council, Ottawa, Ontario K1A 0S2, Canada.

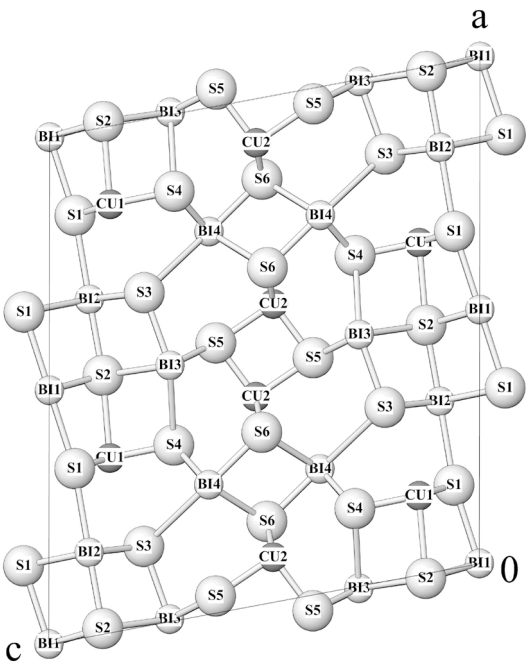

FIG. 2a. Atom positions in cuprobismutite. Axes and orientation as indicated.

DESCRIPTION OF THE STRUCTURES

Modular elements

The crystal structures of the cuprobismutite homologous series can be interpreted (Makovicky 1989) as a regular 1:1 intergrowth on the unit-cell scale of two types of slabs: (a) $(311)_{PbS}$ slabs of a galena-like structure (cuprobismutite-like or kupčíkite-like layers or both), and (b) complex slabs with columns of paired BiS_5 pyramids and paired CuS_4 coordination tetrahedra (thin layer) (Fig. 2). The (a) slabs consist of BiS_6 coordination octahedra, coordination pyramids BiS_5 flanking them, and of the fitting parts of the trigonal coordination bipyramids of Cu(Fe). The (b) layers are identical in all homologues, *i.e.,* homologous accretion takes place in the galena-like portions. In kupčíkite, N = 1, two coordination pyramids of Bi2 attach themselves to the appropriate sides of the Bi1 coordination octahedron; in cuprobismutite, N = 2, there are pairs (Bi2 and Bi3) of such pyramids. The PbS-like slab is then two and three octahedra (or pyramids) wide, respectively. Hodrushite is a regular 1:1 combination of these two slabs thicknesses, N = 1; 2.

The Bi sites

On the polyhedron level, the structures of the cuprobismutite homologous series are distinguished by the presence of regular Bi coordination octahedra, a feature shared, so far, only by the structures of the pavonite homologous series (Makovicky 1989). These octahedra form two groups: (a) the unsubstituted Bi octahedra, Bi1

TABLE 3b. SITE LABELS, OCCUPANCY FACTORS, FRACTIONAL ATOMIC COORDINATES, EQUIVALENT ISOTROPIC AND ANISOTROPIC DISPLACEMENT PARAMETERS FOR HODRUSHITE (FELBERTAL)

site[a]	sof	*x/a*	*y/b*	*z/c*	U_{iso}	U_{11}	U_{22}	U_{33}	U_{13}
*Me*1(Bi)		0.0	0.5	0.0	0.0334(2)	0.0389(4)	0.0276(4)	0.0336(4)	0.0010(3)
*Me*2(Bi)	0.58(4)	0.0	0.0	0.5	0.0334(3)	0.0345(5)	0.0327(6)	0.0329(5)	-0.0005(3)
*Me*2(Ag)	0.42(4)	0.0	0.0	0.5	0.0334(3)	0.0345(5)	0.0327(6)	0.0329(5)	-0.0005(3)
Bi1		0.37147(3)	0.5	0.10117(2)	0.0325(2)	0.0332(2)	0.0326(3)	0.0318(3)	0.0018(2)
Bi2		0.13057(3)	0.5	0.15252(2)	0.0328(1)	0.0330(2)	0.0333(3)	0.0320(3)	0.0002(2)
Bi3		0.17142(3)	0.0	0.29526(2)	0.0314(1)	0.0300(2)	0.0318(3)	0.0324(2)	0.0007(2)
Bi4		0.44186(3)	0.5	0.34474(2)	0.0335(1)	0.0360(2)	0.0323(3)	0.0321(3)	0.0019(2)
Bi5		0.31594(3)	0.0	0.44807(2)	0.0334(1)	0.0332(2)	0.0321(3)	0.0353(3)	0.0050(2)
Cu1A[b]	0.67(2)	0.2028(5)	0.0	0.0266(2)	0.0350(13)	0.0409(32)	0.0334(13)	0.0307(14)	0.0004(17)
Cu1B	0.23(2)	0.1769(11)	0.0	0.0313(5)	0.0350(13)	0.0409(32)	0.0334(13)	0.0307(14)	0.0004(17)
Cu2		0.30651(11)	0.0	0.21181(9)	0.0483(5)	0.0389(9)	0.0405(11)	0.0664(14)	0.0109(9)
Cu3		0.49290(10)	0.0	0.23496(8)	0.0401(4)	0.0356(8)	0.0381(10)	0.0464(10)	0.0005(7)
Cu4		0.12737(15)	0.5	0.42229(8)	0.0525(5)	0.0816(4)	0.0416(12)	0.0332(9)	-0.0104(10)
S1		0.34179(19)	0.0	0.01089(13)	0.0312(6)	0.0324(14)	0.0288(17)	0.0324(15)	0.0017(12)
S2		0.01159(18)	0.0	0.07497(12)	0.0309(6)	0.0320(14)	0.0296(17)	0.0311(15)	0.0025(12)
S3		0.21107(18)	0.0	0.11110(12)	0.0296(6)	0.0298(13)	0.0282(16)	0.0308(14)	0.0026(11)
S4		0.41000(18)	0.0	0.16263(12)	0.0301(6)	0.0321(14)	0.0303(17)	0.0276(14)	-0.0005(11)
S5		0.23697(18)	0.5	0.22278(12)	0.0285(6)	0.0296(13)	0.0252(15)	0.0306(14)	0.0012(11)
S6		0.06358(18)	0.0	0.22780(12)	0.0301(6)	0.0290(13)	0.0295(17)	0.0316(15)	0.0006(11)
S7		0.39101(19)	0.0	0.28721(12)	0.0318(7)	0.0353(15)	0.0325(17)	0.0273(15)	-0.0009(12)
S8		0.09547(18)	0.5	0.34107(13)	0.0308(6)	0.0298(13)	0.0294(17)	0.0335(15)	0.0057(12)
S9		0.29921(18)	0.5	0.37839(12)	0.0302(6)	0.0295(13)	0.0295(17)	0.0316(15)	0.0022(3)
S10		0.46488(19)	0.0	0.43114(12)	0.0317(7)	0.0327(14)	0.0325(18)	0.0298(15)	0.0010(12)
S11		0.15111(20)	0.0	0.46827(13)	0.0341(7)	0.0357(15)	0.0322(18)	0.0342(17)	0.0004(13)

TABLE 4. SELECTED INTERATOMIC Bi–S AND Cu–S DISTANCES (Å) IN THE CUPROBISMUTITE HOMOLOGUES

Cuprobismutite

Bi1		Bi2		Bi3		Bi4		Cu1		Cu2	
S2	2.755(4)	S2	2.681(5)	S5	2.650(4)	S6	2.586(6)	S4	2.265(6)	S5	2.318(6)
S2	2.755(4)	S3	2.739(3)	S5	2.650(4)	S4	2.689(3)	S1	2.339(4)	S6	2.335(3)
S2	2.755(4)	S3	2.739(3)	S3	2.674(5)	S4	2.689(3)	S1	2.339(4)	S6	2.335(3)
S2	2.755(4)	S1	2.952(5)	S2	3.054(5)	S6	3.085(4)	S2	2.878(8)	S5	2.403(7)
S1	2.854(5)	S1	3.031(5)	S2	3.054(5)	S6	3.085(4)				
S1	2.854(5)	S1	3.031(5)	S4	3.383(4)	S3	3.668(5)				
				S4	3.383(4)	S3	3.668(5)				

Hodrushite (Felbertal)

*Me*1		*Me*2		Bi1		Bi2		Bi3		Bi4		Bi5	
S1	2.807(3)	S10	2.759(2)	S2	2.592(3)	S5	2.610(3)	S6	2.575(3)	S7	2.637(2)	S10	2.676(3)
S1	2.807(3)	S10	2.759(2)	S4	2.643(2)	S3	2.692(2)	S8	2.705(2)	S7	2.637(2)	S9	2.731(2)
S2	2.827(2)	S10	2.759(2)	S4	2.643(2)	S3	2.692(2)	S8	2.705(2)	S9	2.705(3)	S9	2.731(2)
S2	2.827(2)	S10	2.759(2)	S1	3.163(3)	S6	3.101(3)	S5	3.040(3)	S10	3.070(3)	S11	2.970(4)
S2	2.827(2)	S11	2.826(4)	S1	3.163(3)	S6	3.101(3)	S5	3.040(3)	S10	3.070(3)	S11	3.036(3)
S2	2.827(2)	S11	2.826(4)	S3	3.452(3)	S2	3.500(3)	S9	3.677(3)	S8	3.340(3)	S11	3.036(3)
				S3	3.452(3)	S2	3.500(3)	S9	3.677(3)	S8	3.340(3)		

Cu1a		Cu1b		Cu2		Cu3		Cu4	
S3	2.291(5)	S3	2.222(14)	S4	2.303(4)	S7	2.333(4)	S8	2.251(4)
S1	2.328(4)	S1	2.286(7)	S5	2.335(2)	S6	2.333(2)	S11	2.351(2)
S1	2.328(4)	S1	2.286(7)	S5	2.335(2)	S6	2.333(2)	S11	2.351(2)
S1	2.497(9)	S1	2.973(20)	S7	2.474(4)	S4	2.392(4)	S10	2.874(4)

Cu-enriched hodrushite (Swartberg)

*Me*1		*Me*2		Bi1		Bi2		Bi3		Bi4		Bi5	
S1	2.800(4)	S10	2.761(3)	S2	2.592(4)	S5	2.601(4)	S6	2.579(4)	S7	2.624(3)	S10	2.648(4)
S1	2.800(4)	S10	2.761(3)	S4	2.641(3)	S3	2.680(3)	S8	2.699(3)	S7	2.624(3)	S9	2.707(3)
S2	2.819(3)	S10	2.761(3)	S4	2.641(3)	S3	2.680(3)	S8	2.699(3)	S9	2.704(4)	S9	2.707(3)
S2	2.819(3)	S10	2.761(3)	S1	3.141(3)	S6	3.110(3)	S5	3.014(3)	S10	3.097(3)	S11	2.964(4)
S2	2.819(3)	S11	2.824(4)	S1	3.141(3)	S6	3.110(3)	S5	3.014(3)	S10	3.097(3)	S11	3.046(3)
S2	2.819(3)	S11	2.824(4)	S3	3.453(3)	S2	3.470(3)	S9	3.724(3)	S8	3.332(3)	S11	3.046(3)
				S3	3.453(3)	S2	3.470(3)	S9	3.724(3)	S8	3.332(3)		

Cu1a		Cu1b		Cu2		Cu3		Cu4		Cu5	
S3	2.326(9)	S3	2.251(7)	S4	2.283(5)	S6	2.315(2)	S8	2.239(5)	S11	2.191(9)
S1	2.351(8)	S1	2.284(3)	S5	2.333(2)	S6	2.315(2)	S11	2.329(3)	S10	2.314(5)
S1	2.353(5)	S1	2.284(3)	S5	2.333(2)	S7	2.327(4)	S11	2.329(3)	S10	2.314(5)
S1	2.353(5)	S1	2.716(6)	S7	2.492(5)	S4	2.365(4)	S10	2.949(5)		

Kupčíkite

Bi1		Bi2		Bi3		Cu1		Cu2		Cu3	
S2	2.803(4)	S1	2.596(4)	S5	2.611(2)	S4	2.308(4)	S3	2.294(3)	S3	2.239(8)
S2	2.803(4)	S4	2.648(2)	S3	2.694(2)	S5	2.340(2)	S2	2.333(2)	S2	2.281(4)
S1	2.825(2)	S4	2.648(2)	S3	2.694(2)	S5	2.340(2)	S2	2.333(7)	S2	2.281(4)
S1	2.825(2)	S2	3.156(3)	S5	3.065(2)	S4	2.437(3)	S2	2.476(6)	S2	3.212(16)
S1	2.825(2)	S2	3.156(3)	S5	3.065(2)						
S1	2.825(2)	S3	3.432(3)	S1	3.476(3)						
		S3	3.432(3)	S1	3.476(3)						

TABLE 3c. SITE LABELS, OCCUPANCY FACTORS, FRACTIONAL ATOMIC COORDINATES, EQUIVALENT ISOTROPIC AND ANISOTROPIC DISPLACEMENT PARAMETERS FOR Cu-ENRICHED HODRUSHITE (SWARTBERG)

site[a]	sof	*x/a*	*y/b*	*z/c*	U_{iso}	U_{11}	U_{22}	U_{33}	U_{13}
*Me*1(Bi)		0.0	0.5	0.0	0.0176(2)	0.0237(4)	0.0130(4	0.0161(4)	0.0027(3)
*Me*2(Bi)	0.750(6)	0.0	0.0	0.5	0.0191(4)	0.0198(4)	0.0212(7)	0.0163(3)	0.0025(4)
Cu5[c]	0.250(6)	0.0266(5)	0	0.4539(3)	0.0191(4)	0.0198(4)	0.0212(7)	0.0163(3)	0.0025(4)
Bi1		0.37068(3)	0.5	0.10071(2)	0.0167(2)	0.0184(4)	0.0182(4)	0.0138(3)	0.0038(2)
Bi2		0.12877(3)	0.5	0.15199(2)	0.0173(2)	0.0188(4)	0.0187(3)	0.0146(3)	0.0026(2)
Bi3		0.16960(3)	0	0.29461(2)	0.0157(2)	0.0153(4)	0.0179(4)	0.0141(3)	0.0023(2)
Bi4		0.44038(4)	0.5	0.34288(2)	0.0185(2)	0.0226(4)	0.0174(3)	0.0157(3)	0.0031(2)
Bi5		0.31627(3)	0.0	0.44844(2)	0.0204(2)	0.0195(4)	0.0223(4)	0.0198(3)	0.0064(2)
Cu1A[b]	0.41(2)	0.2104(4)	0.0	0.02507(26)	0.0234(11)				
Cu1B	0.59(2)	0.1903(3)	0.0	0.02828(19)	0.0234(11)				
Cu2		0.30355(15)	0.0	0.21016(12)	0.0343(6)	0.0283(11)	0.0235(14)	0.0524(17)	0.0187(11)
Cu3		0.49043(13)	0.0	0.23403(09)	0.0232(5)	0.0207(09)	0.0213(12)	0.0278(12)	0.0016(1)
Cu4		0.13079(20)	0.5	0.42145(10)	0.0387(7)	0.0653(19)	0.0287(15)	0.0213(12)	-0.0084(12)
S1		0.34188(23)	0.0	0.01111(15)	0.0152(7)	0.0169(16)	0.0159(20)	0.0132(17)	0.0056(13)
S2		0.01147(22)	0.0	0.07500(15)	0.0148(7)	0.0175(16)	0.0129(19)	0.0142(17)	0.0039(13)
S3		0.20945(21)	0.0	0.11085(15)	0.0147(7)	0.0146(15)	0.0167(20)	0.0128(17)	0.0027(13)
S4		0.40824(22)	0.0	0.16270(14)	0.0133(7)	0.0161(15)	0.0151(19)	0.0089(15)	0.0043(13)
S5		0.23393(21)	0.5	0.22249(14)	0.0131(7)	0.0151(15)	0.0126(19)	0.0119(16)	0.0034(12)
S6		0.06053(22)	0.0	0.22787(16)	0.0153(7)	0.0143(15)	0.0133(19)	0.0181(18)	-0.0006(13)
S7		0.38830(23)	0.0	0.28623(14)	0.0154(8)	0.0198(17)	0.0179(20)	0.0084(16)	0.0002(13)
S8		0.09441(21)	0.5	0.34133(14)	0.0139(7)	0.0161(16)	0.0148(19)	0.0114(16)	0.0052(13)
S9		0.29927(22)	0.5	0.37966(15)	0.0152(7)	0.0154(16)	0.0169(20)	0.0133(17)	0.0025(13)
S10		0.46382(23)	0.0	0.43090(15)	0.0164(8)	0.0178(16)	0.0184(21)	0.0135(17)	0.0057(13)
S11		0.15078(23)	0.0	0.46710(16)	0.0169(8)	0.0184(17)	0.0152(20)	0.0173(19)	0.0029(13)

Notes (applicable to Tables 3a, 3b and 3c): $U_{12} = U_{23} = 0$ by symmetry; sof: site-occupancy factor. a: The site labels follow the structure refinements of synthetic cuprobismutite by Ozawa & Nowacki (1975) and of hodrushite by Kupčik & Makovicky (1968). b: Split position, as in the structure refinement of kupčikite. (Topa *et al.* 2003). c: New split position (this study).

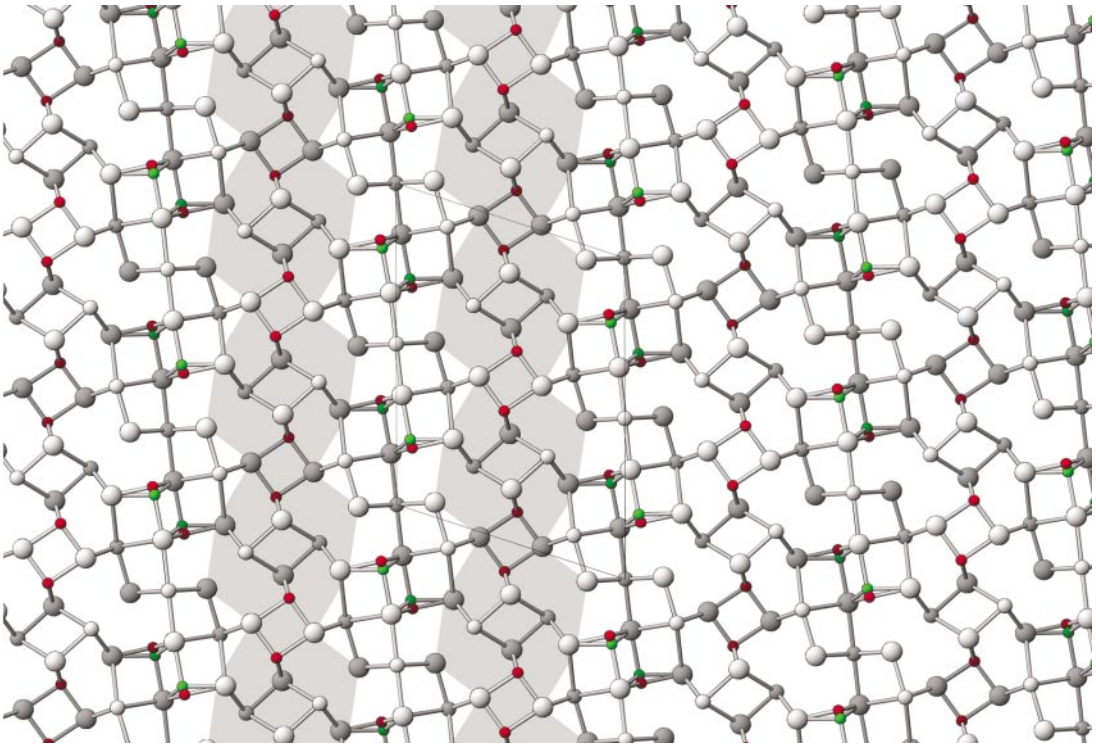

FIG. 3. The crystal structure of kupčíkite $(Cu_{6.58}Fe_{1.28})_{\Sigma 7.86}$ $(Bi_{9.87}Ag_{0.03}Sb_{0.03}Cd_{0.09})_{\Sigma 10.02}$ $S_{20.13}$ from Felbertal (Topa *et al.* 2003). Projection along [010], *a* axis 17.512 Å, *c* axis 12.869 Å. Shaded and void circles indicate two levels of *y*, approximately 2 Å apart. Cu2 (green) represents a mixed Cu,Fe position. Two thin layers (grey-shaded) and one kupčíkite-like layer (unshaded), are indicated.

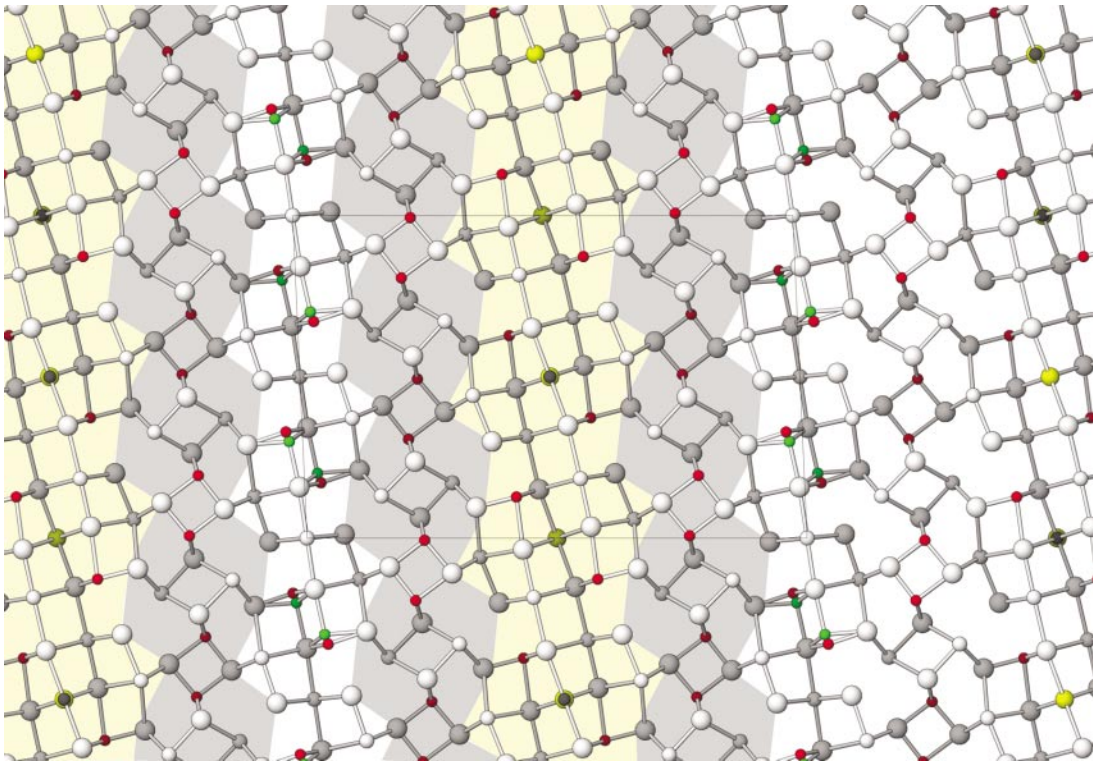

FIG. 4. The crystal structure of hodrushite $(Cu_{7.48}Fe_{0.45})_{\Sigma 7.93}$ $(Bi_{11.54}Ag_{0.40}Pb_{0.08})_{\Sigma 12.02}$ $S_{22.05}$ from Felbertal. Projection along [010], *a* axis 17.562 Å, *c* axis 27.15 Å. Shaded and void circles indicate two levels of *y*, approximately 2 Å apart. Cu1A (green) represents a mixed Cu,Fe position, and *Me*2 a mixed Bi (grey), Ag (yellow) position. Three thin layers (grey-shaded), one kupčíkite-like layer (unshaded), and one cuprobismutite-like layer (yellow-shaded), are indicated.

in cuprobismutite and *Me*1(Bi) in hodrushite, with larger volumes of polyhedron or circumscribed sphere ($93.2 \leq V_s \leq 93.9$ Å^3; for explanations see Appendix), and (b) the Bi octahedra partly substituted by Ag or, in the hodrushite from Swartberg, by Cu with smaller volumes ($V_s = 90.2$ Å^3). For the first group (a), smaller differences in Bi–S bonds are typical (Bi–S 2.80 × 2 and 2.82–2.83 × 4 Å), whereas for the second group (b), larger differences and the opposite bond-length distribution (elongate octahedra, Bi–S 2.76 × 4 and 2.82–2.85 × 2 Å) (Fig. 6) are found.

The next group of Bi polyhedra are BiS_5 coordination pyramids completed to become asymmetric octahedra by an additional Bi–S bond (Bi2 in cuprobismutite, Bi5 in hodrushite). These are attached to the above Bi octahedra only in the thicker, cuprobismutite-like layers. The additional bond is not the longest one in the octahedron: the ratio of shortest bond to additional bond varies from 2.68 Å : 2.95 Å in cuprobismutite to 2.65 Å : 2.97 Å in Cu–Bi-substituted hodrushite. At the same time, the ratio of bonds in the base of the pyramid varies from 2.74 Å : 3.03 Å to 2.71 Å : 3.05 Å.

The last group of Bi polyhedra in the PbS-like layers are the marginal BiS_5 pyramids completed by two additional, equally long bonds to monocapped trigonal prisms (Bi2 in kupčíkite, Bi3 in cuprobismutite, and Bi1 and Bi4 in hodrushite). The asymmetry of Bi2 coordination in kupčíkite is close to that in the corresponding Bi1 in hodrushite; the same holds for the asymmetry of the Bi3 coordination in cuprobismutite in relation to that of Bi4 in hodrushite (Table 5).

There are systematic differences between kupčíkite and cuprobismutite in the coordination of bismuth in columns of paired pyramids in the (b) slabs (Bi3 and Bi4 in the above order). Bi4 in cuprobismutite has a greater asymmetry of coordination, *e.g.*, the ratio of the pyramid height to the longest bonds below the pyramid is 2.61Å : 3.48Å in kupčíkite, whereas it is 2.59Å : 3.67Å in cuprobismutite. Remarkably, this trend is maintained in hodrushite. Pyramids of Bi2 situated next to the kupčíkite-like slabs tend toward a configuration of kupčíkite type, and those of Bi3 adjacent to cuprobismutite-like slabs assume cuprobismutite-like configurations (Table 4, Figs. 3, 4).

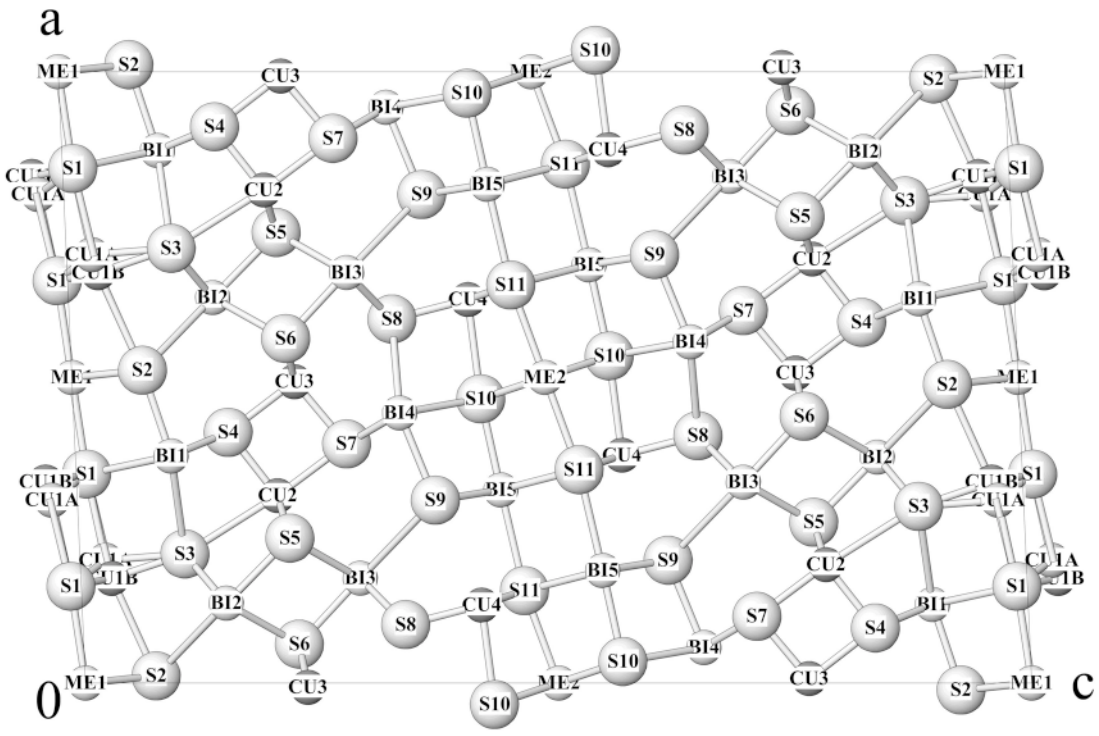

FIG. 4a. Atom positions in hodrushite. Axes and orientation as indicated.

The above trends in configuration can best be expressed by the volume-based eccentricity (see the Appendix and Table 5) of Bi polyhedra: 0.0 for the regular coordination octahedra [*e.g.*, *Me*1(Ag,Bi) and *Me*2(Bi) in hodrushite], 0.24–0.26 for the attached asymmetric octahedra (such as Bi5 in hodrushite), 0.41–0.42 for the marginal monocapped trigonal prisms of Bi (*e.g.*, Bi4 in hodrushite), 0.55 for the cuprobismutite-like monocapped-prismatic configuration in the columns of paired coordination pyramids of Bi (Bi3 in hodrushite), and 0.5 for the kupčíkite-like configuration in the latter (Bi2 in hodrushite).

Further details of the coordination of Bi can be seen in the diagrams of volume-based sphericity *versus* volume-based eccentricity of the coordination polyhedra of Bi (Fig. 7a), and of the hyperbolic correlation of the opposing Bi–S bonds distances (Fig. 8). In general, there is an inverse correlation between eccentricity and sphericity of the bismuth polyhedra in Figure 7a, violated only by the shapes of partly substituted bismuth octahedra denoted as Bi1 in cuprobismutite and *Me*2 in hodrushite (the two lowermost values of sphericity at zero eccentricity in Fig. 7a). The polyhedra with greatest eccentricity thus also deviate most from regularity. The types of bismuth polyhedron defined above are clearly distinguished in Figure 7a, whereas there is coincidence of these properties for the same site in different homologues. Differences between the kupčíkite-like and cuprobismutite-like environments for Bi coordinations in the double-pyramid columns of the (b) slabs are more pronounced than those between the marginal Bi atoms in the (a) slabs and in the (b) slabs.

The same clear-cut distribution of polyhedron types is found in the diagram of volumes V_p of coordination polyhedra *versus* volumes V_s of spheres circumscribed by least-squares fitting to these polyhedra (Fig. 7b). Regular or asymmetrical octahedra offer considerably smaller volumes to Bi and its lone-pair electrons than do capped trigonal prisms; the degree of the Ag-for-Bi substitution is reflected in the reduced volume of the substituted octahedra. Volumes of prisms increase from cuprobismutite-like slabs, through kupčíkite-like slabs to those in paired columns. Interestingly enough, the largest volumes are those for paired prisms close to cuprobismutite columns, which also display the largest distortion.

Coordination polyhedra of the bismuth in cuprobismutite homologues follow closely a hyperbolic correla-

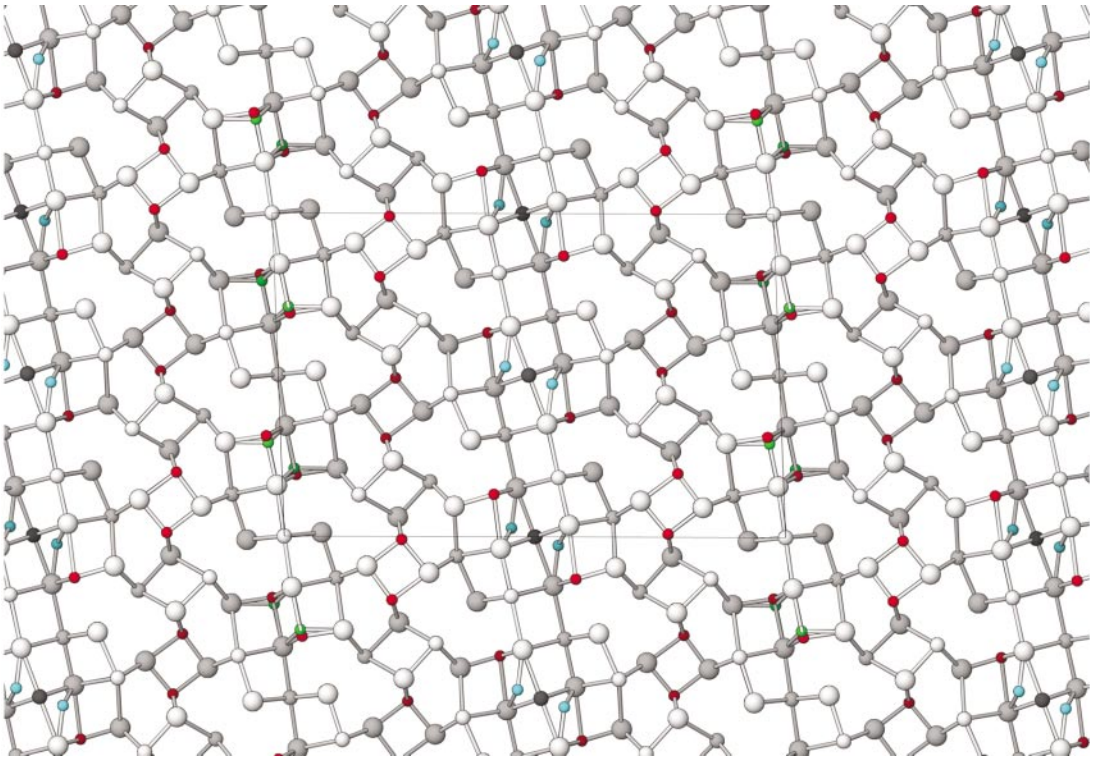

FIG. 5. The crystal structure of Cu-enriched hodrushite $(Cu_{7.72}Fe_{0.28})_{\Sigma 8.00}Cu_{0.36}(Bi_{11.51}Ag_{0.03}Pb_{0.08}Sb_{0.03}Cd_{0.08})_{\Sigma 11.73}S_{21.91}$ from Swartberg, South Africa. Projection along [010], *a* axis 17.535 Å, *c* axis 27.109 Å. Shaded and void circles indicate two levels of *y*, approximately 2 Å apart. Cu1A (green) represents a mixed Cu,Fe position. Cu5 (blue) and *Me*2(Bi) (dark grey) denote the new split position.

tion of opposing bonds, investigated originally by Trömel (1981) for Sb^{3+}, Te^{4+}, I^{5+} bonds with oxygen, and by Berlepsch *et al.* (2001) for bismuthinite derivatives (meneghinite homologues). Bismuth Bi^{3+} is the only case among Group-V elements for which an octahedral coordination with a 1:1 ratio of opposing bonds exists. The unsubstituted Bi octahedra cluster tightly around the hyperbola, whereas the values above or below the hyperbola belong to the partly substituted octahedra (Fig. 8). Numerical data for the hyperbola fitted to the bond lengths in the three substituted structures are presented in Table 6, together with those obtained by Berlepsch *et al*. (2001) for literature data on bismuthinite derivatives.

Irrespective of their orientation in the PbS-like (a) slabs, or of their position in the (b) layers, pairs of opposing Bi–S distances in kupčíkite (N = 1) and the kupčíkite-like module in hodrushite lie closer to the hyperbola than do those from cuprobismutite (N = 2) and the cuprobismutite-like portions of the hodrushite. The values for the cuprobismutite-like slab (Bi4 and Bi5 in hodrushite) accompany the hyperbola from both sides; the trends for the bond pairs oriented across the PbS-like slabs and those for the bond pairs oriented nearly parallel to the slabs cross on the 1:1 point (Fig. 8). This cross-correlation of the Bi–S bond scheme suggests that a compensation of strains and stresses across and along the slabs may be present in the thicker, cuprobismutite-like slabs of the cuprobismutite homologues. These phenomena are largely absent from the thinner, kupčíkite-like slabs.

The Cu sites

In all structures, the tetrahedral coordination of copper is asymmetrical, transitional to trigonal-planar or, considering more distant ligands, trigonal-bipyramidal (Figs. 2, 3). The trend of coordination asymmetry for copper tetrahedra in the (b) slab is opposite that for Bi in paired pyramids. The asymmetry of coordination is greater for the kupčíkite-like configuration (the volume-based eccentricity for Cu1 in kupčíkite is 0.12, and in the range 0.16–0.19 for Cu2 in hodrushite), whereas it is smaller for cuprobismutite-like configurations (the ec-

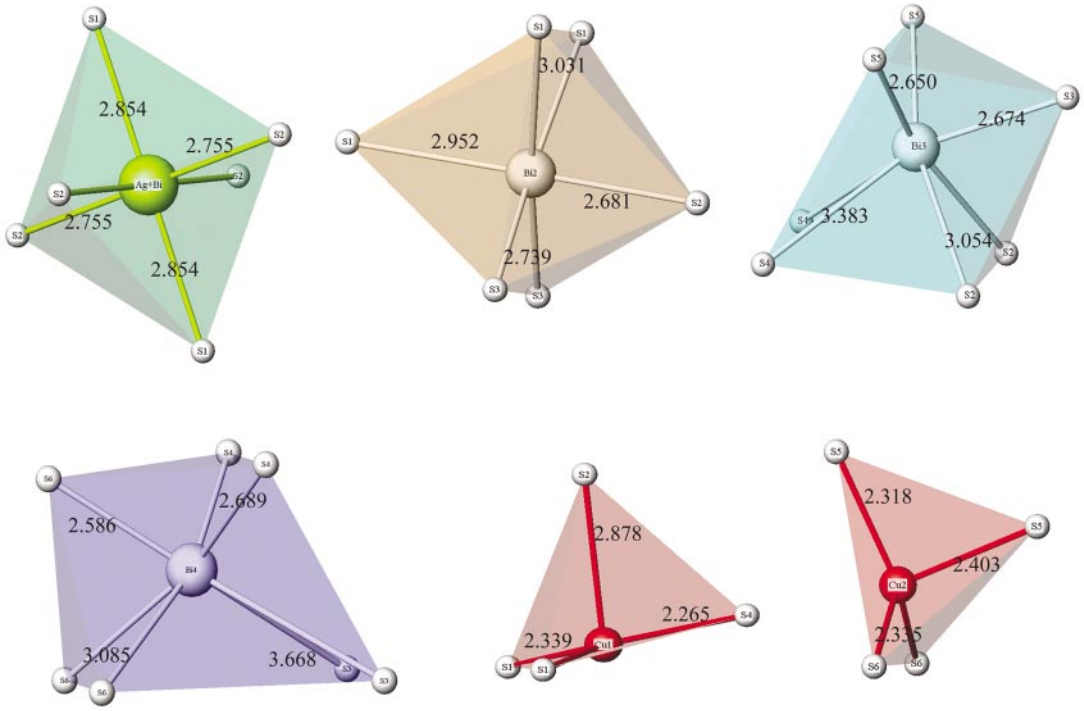

FIG. 6. Bi and Cu coordination polyhedra in cuprobismutite.

centricity value for Cu2 in cuprobismutite is 0.08, and in the range 0.05–0.06 for Cu3 in hodrushite).

In all structures, the galena-like slabs are flanked by trigonal bipyramidal voids accommodating copper ± iron. The latter could be refined as split position in the case of kupčíkite-like slabs, whereas refinements yielded only single positions for the cuprobismutite-like slabs. As discussed by Topa *et al.* (2003) for kupčíkite, splitting of the position is not automatically a consequence of Fe-for-Cu substitution: this splitting also is found in $Cu_4Bi_4S_9$ (Bente & Kupčik 1984) and $Cu_4Bi_4Se_9$ (Makovicky *et al.* 2002) in a completely analogous situation.

Both in kupčíkite and in kupčíkite-like $N = 1$ slabs of the hodrushite structure, the splitting produces a nearly triangular planar position (Cu3 in kupčíkite and Cu1B in hodrushite) and a distorted tetrahedral position (Cu2 and Cu1A, respectively). In the trigonal bipyramidal void of kupčíkite, distances to the distal vertices are 2.93 Å and 3.21 Å for Cu3, whereas they are 2.48 Å *versus* 3.66 Å for Cu2. The Cu–S distances (Table 4) indicate clearly CN = 3 and CN = 4, respectively. Topa *et al.* (2003) placed Fe^{3+} in kupčíkite at the tetrahedral Cu2 position; the same can be assumed for the Cu1A site in hodrushite.

The single site Cu1 in cuprobismutite is closer to the triangular planar site seen in the split configuration; the same is true for the Cu4 position of cuprobismutite-like slabs in hodrushite, especially in the Cu-enriched variety (Table 4). The augmented displacement-factor U_{11} suggests pronounced displacements of these atoms in the direction perpendicular to the triangular plane. The differences in coordination between the triangular and tetrahedral sites are best seen in the eccentricity values of the tetrahedra in Table 5.

THE SUBSTITUTING ELEMENTS

Silver is concentrated in cuprobismutite (Tables 1, 2) at the Bi1 position, which contains 0.292 Bi + 0.708 Ag. Silver has been placed on (0,½,0) overlapping with Bi without altering its displacement factors (Table 3a). In hodrushite, with less Ag, the corresponding *Me*2 position contains 0.58Bi + 0.42Ag (Table 3b); the influence on the coordination has already been described.

In Cu-enriched hodrushite, this polyhedron consists of 0.75Bi, flanked by triangular Cu5 on the two free faces of the Bi octahedron; the composite occupancy is 0.5 Cu, and the bonds correspond well to triangular Cu when taking into account that the S sites in three quar-

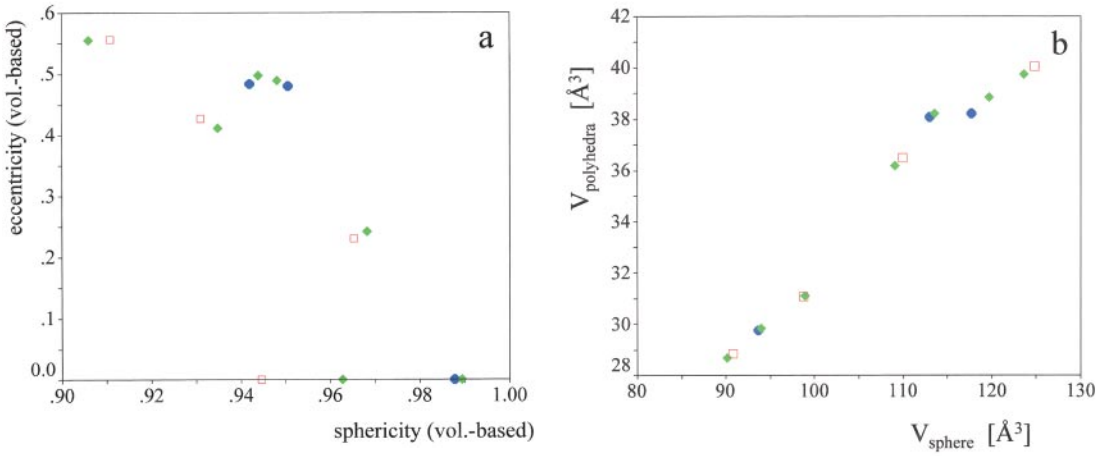

FIG. 7. Polyhedron characteristics of Bi coordination polyhedra in cuprobismutite homologues. (a) Volume-based eccentricity *versus* volume-based sphericity, (b) polyhedron volume *versus* circumscribed-sphere volume. Symbols: cuprobismutite (□), hodrushite (◇), kupčíkite (○).

TABLE 5. POLYHEDRON CHARACTERISTICS FOR REFINED STRUCTURES OF MEMBERS OF THE CUPROBISMUTITE SERIES

	Volume-based eccentricity	Sphere radius Å	Sphere volume Å^3	Volume-based sphericity	Polyhedron volume Å^3	Volume distortion
Cuprobismutite						
Bi1	0.0000	2.788	90.752	0.9446	28.854	0.0011
Bi2	0.2309	2.867	98.741	0.9653	31.073	0.0114
Bi3	0.4275	2.972	109.987	0.9310	36.489	0.1233
Bi4	0.5568	3.100	124.801	0.9109	40.064	0.1517
Cu1	0.5146	2.386	56.886	1.0000	6.761	0.0299
Cu2	0.0819	2.341	53.729	1.0000	6.324	0.0394
Hodrushite (Felbertal)						
*Me*1	0.0000	2.820	93.948	0.9894	29.845	0.0020
*Me*2	0.0001	2.782	90.164	0.9627	28.679	0.0007
Bi1	0.4899	3.004	113.546	0.9482	38.217	0.1105
Bi2	0.4972	3.057	119.666	0.9439	38.843	0.1422
Bi3	0.5554	3.090	123.633	0.9060	39.755	0.1502
Bi4	0.4118	2.964	109.073	0.9349	36.177	0.1235
Bi5	0.2425	2.869	98.892	0.9681	31.096	0.0121
Cu1A	0.1791	2.351	54.451	1.0000	6.611	0.0090
Cu1B	0.6051	2.351	54.451	1.0000	6.611	0.0090
Cu2	0.1618	2.345	54.049	1.0000	6.353	0.0406
Cu3	0.0629	2.342	53.806	1.0000	6.340	0.0383
Cu4	0.5171	2.384	56.789	0.9999	6.729	0.0329
Hodrushite (Swartberg)						
*Me*1	0.0000	2.813	93.225	0.9891	29.611	0.0021
*Me*2	0.0000	2.782	90.182	0.9648	28.687	0.0007
Cu5	0.3472	2.254	47.958	1.0000	0.000	0.0000
Bi1	0.4877	2.997	112.806	0.9425	37.985	0.1102
Bi2	0.4954	3.046	118.334	0.9508	38.453	0.1413
Bi3	0.5695	3.097	124.454	0.8894	39.778	0.1554
Bi4	0.4194	2.962	108.822	0.9446	36.079	0.1239
Bi5	0.2657	2.860	97.964	0.9652	30.741	0.0142
Cu1A	0.0248	2.346	54.068	1.0000	6.570	0.0082
Cu1B	0.4056	2.346	54.068	1.0000	6.570	0.0082
Cu2	0.1934	2.339	53.626	1.0000	6.282	0.0439
Cu3	0.0489	2.326	52.718	0.9999	6.211	0.0384
Cu4	0.5834	2.372	55.923	0.9999	6.633	0.0319
Kupčikite						
Bi1	0.0000	2.871	93.686	0.9877	29.754	0.0022
Bi2	0.4804	2.999	112.988	0.9505	38.081	0.1093
Bi3	0.4839	3.040	117.665	0.9420	39.223	0.1415
Cu1	0.1213	2.343	53.901	1.0000	6.287	0.0479
Cu2	0.1574	2.350	54.354	1.0000	6.596	0.0096
Cu3	0.5743	2.270	48.780	1.0000	6.596	0.0096

TABLE 6. CHARACTERISTIC CONSTANTS FOR THE ELEMENT-SPECIFIC BOND-LENGTH HYPERBOLAE OF OPPOSING Bi–S DISTANCES *x* AND *y* IN CATION POLYHEDRA IN THE CUPROBISMUTITE SERIES

Atom	*a* [Å]	*c* [Å^2]	R^2	D_{min} [Å]	$D_{(x=y)}$ [Å]
Bi[1]	2.538	0.0754	0.988	2.538	2.813
Bi[2]	2.543	0.0707	0.998	2.543	2.808

[1] Bi in meneghinite homologues, after Berlepsch *et al.* (2001).
[2] This study.

ters of cases belong to the Bi octahedron and not to Cu triangles (Table 4).

As already mentioned above, iron has been ascribed to the distorted tetrahedrally coordinated sites situated in the split trigonal bipyramidal sites. Assigning lead to the bismuth sites is most difficult. With about 0.10–0.15 Pb *apfu* (atoms per formula unit) in kupčíkite and hodrushite, and ~0.25 Pb *apfu* in cuprobismutite, this task is virtually impossible.

COMPOSITIONAL VARIATIONS AND CRYSTAL CHEMISTRY

Calculation of N, the order of the homologue

Calculation of the order *N* of a cuprobismutite homologue (see Appendix) in a way similar to the calculation of *N* in the lillianite homologous series (Makovicky & Karup-Møller 1977) only becomes possible now, on the basis of results of structural refine-

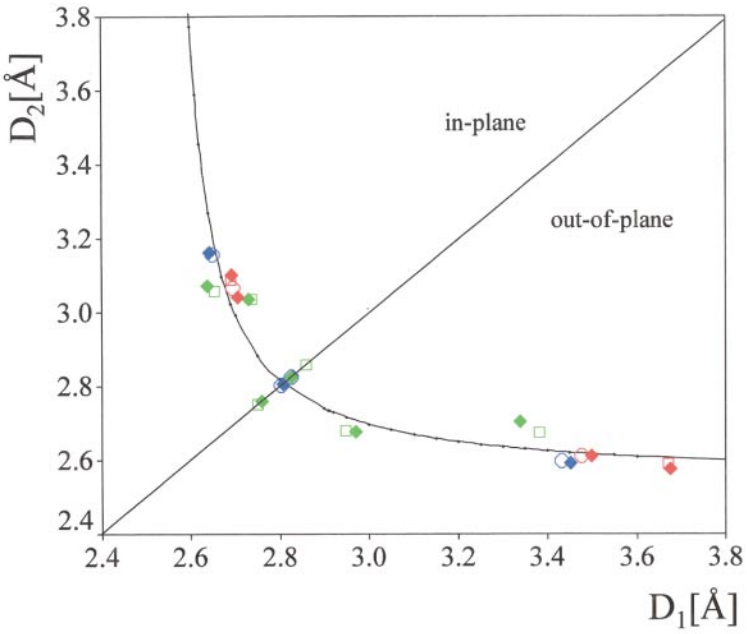

FIG. 8. Hyperbolic correlation of opposing Bi–S bond distances in cuprobismutite homologues. Symbols distinguish the phases studied as well as the kupčíkite-like, cuprobismutite-like (a) slabs (module), and the composite (b) slabs (thin layer) interleaved with them. Symbols: blue circle: kupčíkite – kupčíkite modules, blue diamond: hodrushite – kupčíkite modules, green diamonds: hodrushite – cuprobismutite modules, green squares: cuprobismutite – cuprobismutite modules, red circle: kupčíkite thin layer, red diamond: hodrushite thin layer, red square: cuprobismutite thin layer.

ments for kupčíkite (Topa *et al.* 2003), cuprobismutite and hodrushite (current work). The reasons are twofold.

a) The ratio of Cu sites *versus* Bi sites in the structure. Wherever the structure requires partial substitution of Bi by Cu in order to reduce the total cation charges (as typified by synthetic cuprobismutite: Ozawa & Nowacki 1975), the Cu:Bi ratio does not reflect the ratio of fundamentally distinct Cu and Bi sites, and erroneous values of N result. The substitution is governed by a combination of the charge-balance requirement with steric problems encountered in the structure, so that a ratio of 3Cu for 1Bi cannot be expected to occur. The stoichiometry of $N = 1$, synthetic $Cu_4Bi_5S_{10}$ (Mariolacos *et al.* 1975), suggests that even some Cu^{2+} may be present in the structures in addition to Cu^{+}, *i.e.*, *a priori* assumptions cannot always be made about the valence of Cu.

b) Until the recent determinations of the structures, the structural role of two principal substituting elements, Fe and Ag, and the degree of Cu-for-Bi substitution in natural phases, were not known.

The structural-site formula for kupčíkite, $N = 1$, is 'Cu_8''Bi_{10}'S_{20}; that for cuprobismutite, $N = 2$, is 'Cu_8''Bi_{14}'S_{24}, resulting in a general formula 'Cu_8''$Bi_{10+4(N-1)}$'S_{4N+16}. For N based on metal ratios, this formula yields $N = 2\bullet$('Bi'/'Cu') – 1.5, where 'Bi' and 'Cu' can be atom percentages or atoms per (a suggested) formula unit, with 'Bi' = Bi + Sb + Ag + Pb + Cd and 'Cu'= Cu + Fe, *i.e.*, we take into account the site occupancies without regard to element valences. The successful tests of these calculations, including the cases confirmed by structure determination (Fig. 9), suggest a general validity of the proposed substitutions and the virtual absence of important Cu-for-Bi substitution in the samples studied. Only one natural case, hodrushite from Swartberg, South Africa, contains important amount of Cu substituting for Bi. This results in an erroneously low N value for this sample ($N = 1.27$), in contradiction of the $N = 1.5$ confirmed by structure determination. If a chemical N is calculated for synthetic cuprobismutite, $Cu_{10.44}Bi_{12.4}S_{24}$ with considerable substitution of Cu for Bi at several positions, (Ozawa & Nowacki 1975), the resulting value is $N = 0.9$, instead of the expected 2.0.

Compositional variations

The three known phases of the series are clearly separated in the three-component discrimination diagrams shown in Figures 10a–c, although in two of these

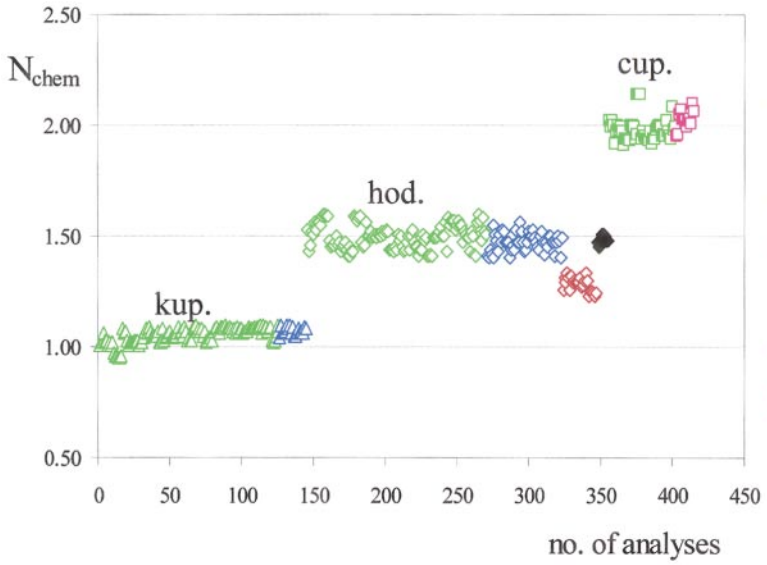

FIG. 9. Calculated values of homologue order *N* for the members of the cuprobismutite homologous series studied (based on microprobe data). *N* = 1 is kupčíkite, *N* = 1.5, hodrushite, and *N* = 2, cuprobismutite. Anomalous results for hodrushite from Swartberg are explained in the text. Symbols: green triangles: kupčíkite from Felbertal, blue triangles: kupčíkite from Băiţa Bihor, green diamonds: hodrushite from Felbertal, blue diamonds: hodrushite from Băiţa Bihor, brown diamonds: hodrushite from Swartberg, black diamonds: hodrushite from Hodrusha, green squares: cuprobismutite from Felbertal, magenta squares: cuprobismutite from Ocna de Fier.

they span only a small area. These diagrams work very well for the substituted phases, whereas the Cu-enriched hodrushite (and with it all potential unsubstituted phases) is a notable exception. The (Cu + Fe) – (Bi + Ag + Pb) – S diagram (Fig. 10a) describes the site ratios in these homologues. It demonstrates that additional Cu sites are present in the phases with limited extents of Fe, Ag, and Pb substitution for the principal elements, such as the Cu-enriched hodrushite just mentioned. The Fe–Pb–Ag diagram (Fig. 10b) describes the ratios of principal substituting elements (*i.e.*, ratios of principal charge-balancing processes). The (Cu + Fe) – (Bi + 0.5Pb) – (Ag + 0.5Pb) plot (Fig. 10c) combines the properties of the two above diagrams.

Our crystallographic studies indicate that four types of cation substitutions are present in the cuprobismutite homologues: (a) Cu-for-Bi, (b) Ag-for-Bi, (c) Pb-for-Bi, and (d) Fe^{3+}-for-Cu. The details of the complicated crystal chemistry of the cuprobismutite homologous series are best resolved in a series of binary diagrams (Figs. 11a–h) combined with the Fe–Pb–Ag diagram (Fig. 10b). The binary diagrams are based on number of atoms per respective formula units. They combine changes in the formulae with substitutional trends.

The (Cu + Fe) *versus* Bi diagram (Fig. 11a) shows displacement of Bi values from the ideal values of 10, 12, and 14 *apfu*, respectively. These displacements correlate well with the Ag and Pb substitutions in the individual compounds (Figs. 11d, f); these substitutions increase from kupčíkite to cuprobismutite. The formulae used for calculation of atomic percent values in Figures 11a–h should ideally deliver 8(Cu + Fe) *apfu*. Hodrushite has (Cu + Fe) contents balanced about the value of 8 *apfu*, whereas cuprobismutite has a slight surplus above 8 *apfu*, with the increase in Cu matched by a decrease in Bi, an indication of a small degree of Cu-for-Bi substitution. Copper-enriched hodrushite shows a decrease in Bi contents and a substantial increase in Cu content in comparison with the Fe–Ag–Pb-substituted variety of hodrushite. Kupčíkite shows a small deficit in (Cu + Fe) (Fig. 11a), apparently due to 0.1 Pb substituting for Bi in the Felbertal material, and also to higher content of Fe^{3+} (Fig. 11c). A charge-balance calculation shows that both kupčíkite samples analyzed show excellent charge-balance if Cu^{+} and Fe^{3+} are assumed to be present.

The presence of only minor Cu-for-Bi substitution in the Ag–Fe–Pb-substituted homologues is confirmed by the closeness of the calculated values of *N* to the ideal ones (Fig. 9) and by a well-expressed clustering of compositional points in Figure 10a.

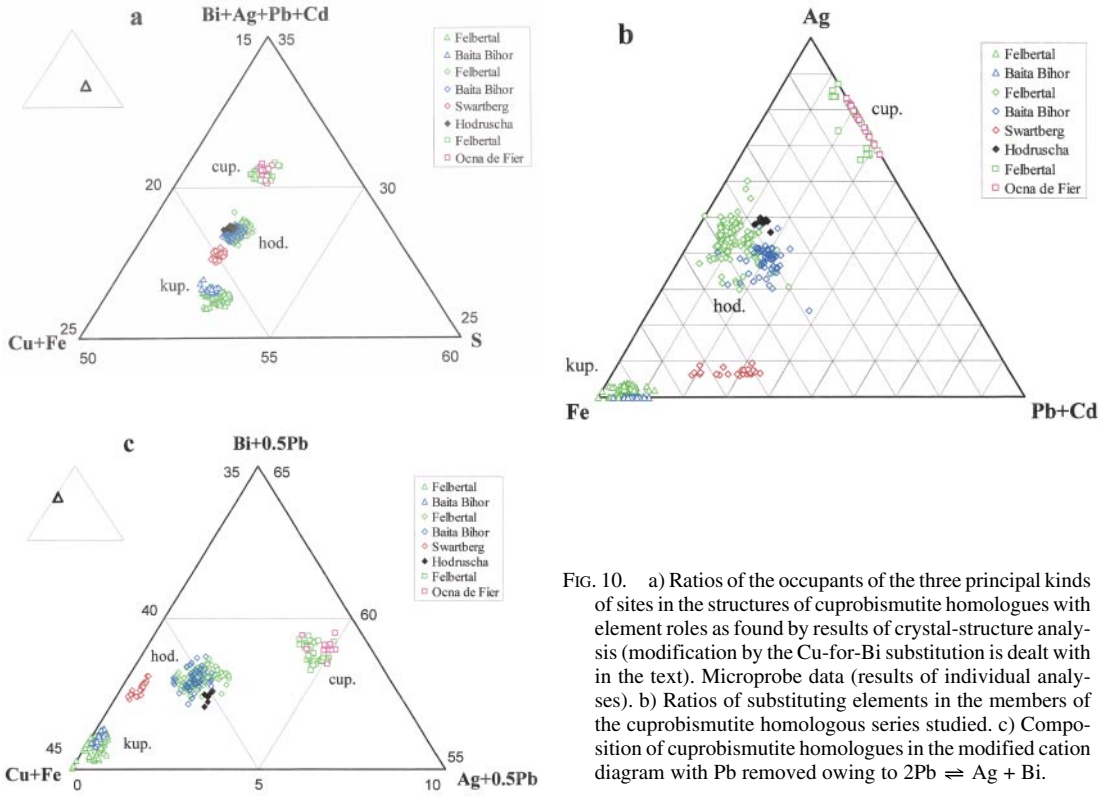

FIG. 10. a) Ratios of the occupants of the three principal kinds of sites in the structures of cuprobismutite homologues with element roles as found by results of crystal-structure analysis (modification by the Cu-for-Bi substitution is dealt with in the text). Microprobe data (results of individual analyses). b) Ratios of substituting elements in the members of the cuprobismutite homologous series studied. c) Composition of cuprobismutite homologues in the modified cation diagram with Pb removed owing to $2Pb \rightleftharpoons Ag + Bi$.

Figure 10b shows that the amounts of Fe-for-Cu and Ag-for-Bi substitutions are balanced in the hodrushite samples, whereas only a single type of substitution plays an appreciable role in the members with $N = 1$ and $N = 2$. Figures 11b and 10b show that hodrushite aggregates from Felbertal and Băiţa Bihor show compositional trends toward the unsubstituted hodrushite, with the increasing role of Fe-for-Cu and Pb-for-Bi substitutions correlated with a decreasing role of Ag-for-Bi substitution. The Ag-enriched type of hodrushite material from Hodrusha does not follow this trend. For cuprobismutite, $N = 2$, the outlines of the composition field in Figure 11b indicate trends similar to those of hodrushite from Felbertal. Only in cuprobismutite is a distinctly negative correlation between Bi and Ag contents observed (Fig. 11d).

All four types of substitution show mutual correlations. The weakest correlation takes place between Pb(+ Cd) and Fe (Fig. 11h). More pronounced trends are: (a) negative correlations between Ag and Cu + Fe contents in hodrushite and cuprobismutite (an interplay between the Ag-for-Bi and Cu-for-Bi substitutions) in Figure 11b; (b) a fan of trends for hodrushite in the Ag *versus* Fe diagram (Fig. 11e), with the majority of cases following an approximate 2Ag:1Fe line (a consequence of the fact that the increase in the extent of Fe-for-Cu substitution must be compensated by the Ag-for-Bi substitution). The other potential mechanism of compensation, (c) the Pb(+ Cd)-for-Bi substitution, is discernible for hodrushite (Fig. 11f). (d) The indistinct negative 1:1 correlation between Pb and Ag contents (Fig. 11g) suggests that Pb(+ Cd) and Ag compete for the same sites in hodrushite and cuprobismutite. For hodrushite, the 2:1 trend, *i.e.*, the $Ag + Bi \rightleftharpoons 2Pb$ substitution, is suggested by certain groups of data within the broad cluster of data points in Figure 11g. This factor explains the lack of correlation between the Bi and Ag contents in hodrushite in Figure 11d, which is at variance with the case for cuprobismutite.

The observed trends are not limited to a combination of data from different localities; the richest spectrum of trends and correlations is observed within one locality, the Felbertal deposit (Figs. 11a–h), where it expresses the variations within single grains and their aggregates.

Summarizing these data for individual phases, *kupčíkite* from Felbertal displays a small (0.1 *apfu*) deficit in Bi, related to a weak Pb-for-Bi and very weak Ag-for-Bi substitution. A high level of Fe^{3+}-for-Cu substitution (~1.2 Fe *apfu*) was observed (Fig. 11c), in

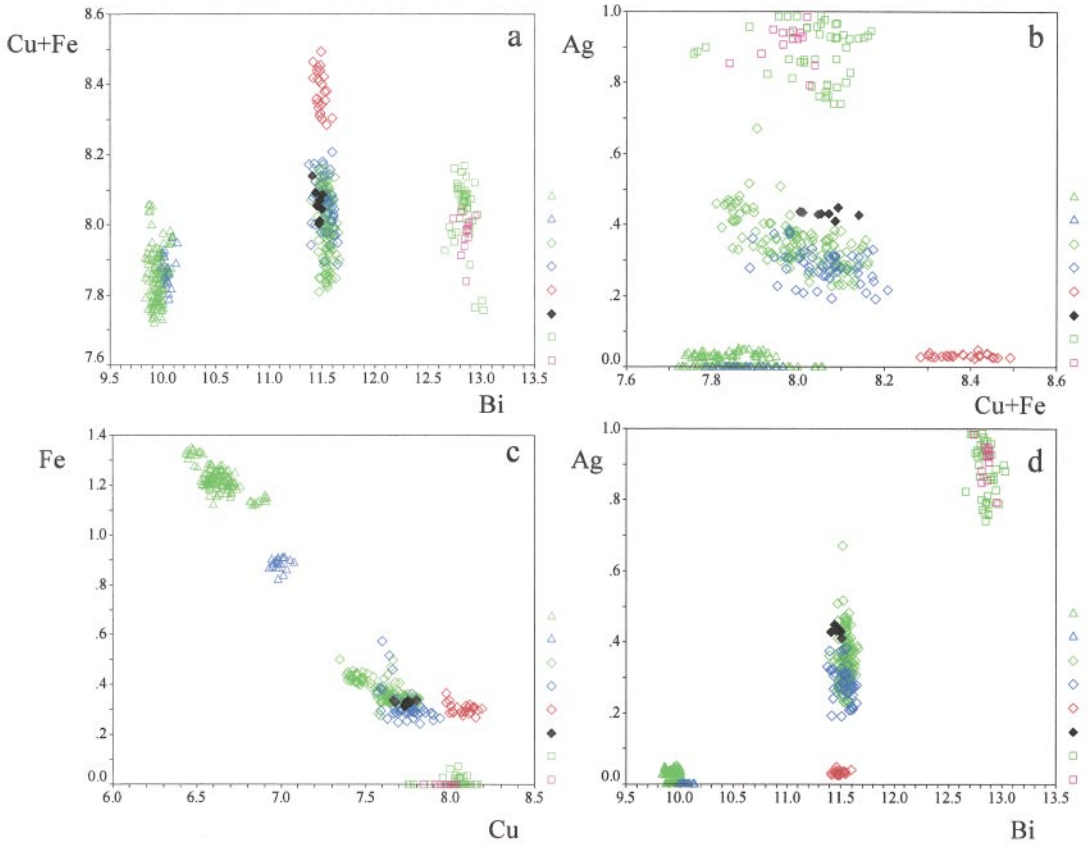

FIG. 11. Element-correlation diagrams for the members of the cuprobismutite homologous series studied. The number of atoms per formula unit were calculated from electron-microprobe data (details in the text). Symbols and colors as in Figures 9 and 10.

comparison with *kupčíkite* from Băiţa Bihor (~0.9 Fe *apfu*). It correlates with a small deficit in Cu (Fig. 11a).

Cuprobismutite only exceptionally has measurable contents of Fe (Fig. 11c). The extent of Ag-for-Bi substitution reaches 1 *apfu*, although values as low as 0.75 *apfu* also are common (Fig. 11d). Pb(+ Cd)-for-Bi substitution plays an important role, Ag and Pb(+ Cd) competing for the sites in the PbS-like layers. Negative correlations exist between Pb(+ Cd), Ag, and (Cu + Fe) *versus* Bi. The broad negative correlation between Ag and (Cu + Fe) suggests a competition between the (Cu + Fe)-for-Bi and Ag-for-Bi mechanisms.

Hodrushite combines the trends observed in $N = 1$ and $N = 2$ homologues. Negative correlation between Bi and (Cu + Fe) is weak, best observable for the Pb(+ Cd)- and Ag-free varieties; the negative correlation is distinct in the plot Pb(+ Cd) *versus* Bi, but not in the plot of Ag *versus* Bi, suggesting an important role of the Ag + Bi $\rightleftharpoons$ 2Pb substitution in the Felbertal and Băiţa Bihor materials. The extent of replacement of Bi by other cations is substantial, reducing the number of Bi *apfu* from 12 to below 11.6. The Cu-for-Bi substitution competes with the Ag-for-Bi substitution. The extent of the Fe-for-Cu substitution increases in parallel with that of the Ag-for-Bi substitution. Although less distinctly, it decreases with the Pb(+ Cd)-for-Bi substitution. The type hodrushite from Hodrusha is relatively enriched in Ag and modestly so in Pb (matching the Cu-enriched variety from Swartberg in its Pb contents); only average Fe contents and non-negligible Cu-for-Bi substitution are observed in this sample.

CONCLUSIONS

(1) Crystal structures of natural cuprobismutite and two types of hodrushite were refined and chemical variations for eight samples of cuprobismutite homologues from five localities were determined. The new data allow a crystal-chemical evaluation of element substitutions observed in natural samples.

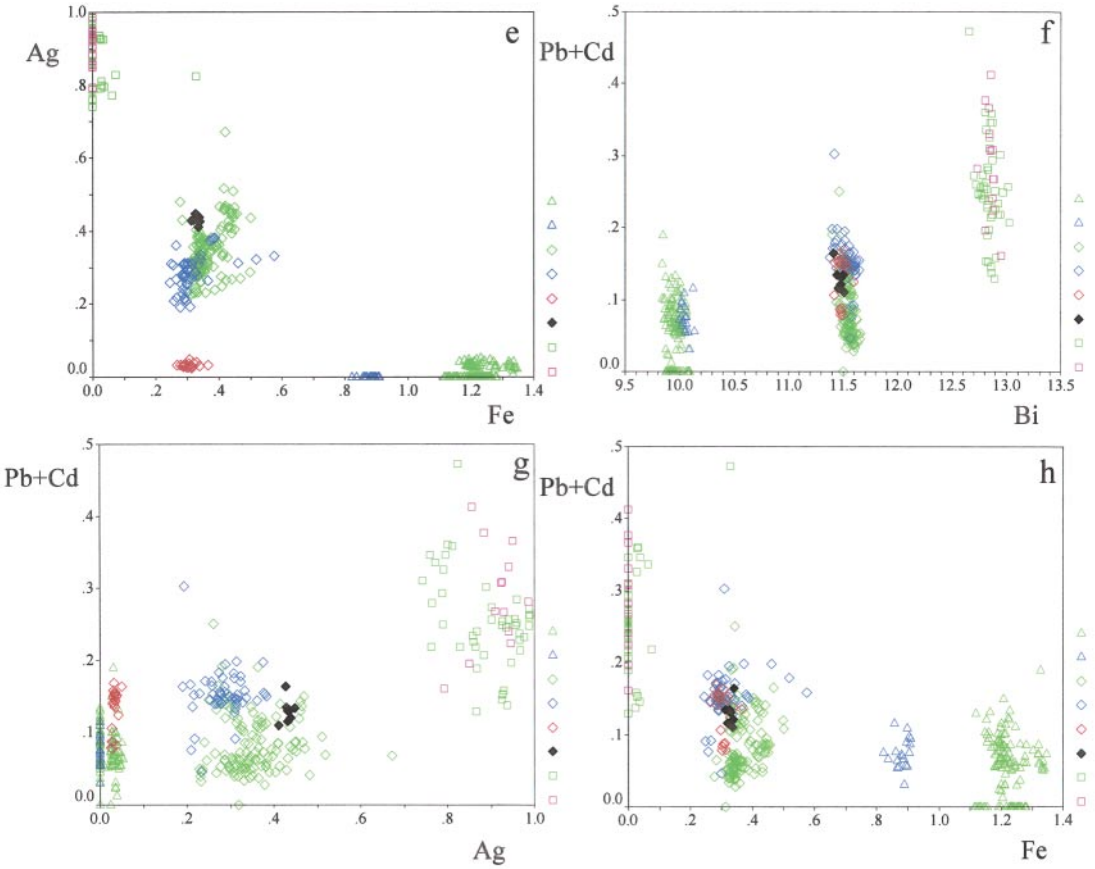

(2) The crystal structures of cuprobismutite homologues are composed of accretional PbS-like (a) slabs in two distinct thicknesses (kupčíkite-like $N = 1$ and cuprobismutite-like $N = 2$ slabs) interleaved by (b) slabs composed of columns of paired Bi pyramids and Cu tetrahedra.

(3) Four types of Bi polyhedra are present in cuprobismutite homologues: central Bi octahedra in the PbS-like slabs, asymmetrically distorted octahedra and capped trigonal prisms in these slabs as well as paired capped trigonal prisms in the (b) slabs. These groups have very distinct coordination properties, polyhedron volumes and eccentricities.

(4) Copper occurs in paired coordination tetrahedra in (b) slabs and as split trigonal planar or tetrahedral coordination in trigonal bipyramidal spaces lining the (a) slabs.

(5) Silver substitutes for Bi in coordination octahedra of the cuprobismutite-like ($N = 2$) layers; minor amounts of Pb probably do as well; Fe^{3+} substitutes for tetrahedrally coordinated Cu along the boundaries of kupčíkite-like ($N = 1$) (a)-type slabs. In hodrushite from Swartberg, ^{III}Cu substitutes for a part of ^{VI}Bi in the thicker slabs. Multiple correlations among these substitutions are documented by electron-microprobe data.

Acknowledgments

This project was supported by grants of the State Research Council of Denmark and by a grant to D. Topa by the University of Salzburg. The manuscript benefitted from comments of P. Goodell and an anonymous referee, as well as from the editorial care of Robert F. Martin.

References

Balić-Žunić, T. & Makovicky, E. (1996): Determination of the centroid or "the best centre" of a coordination polyhedron. *Acta Crystallogr.* **B52**, 78-81.

_____ & Vicković, I. (1996): IVTON – program for the calculation of geometrical aspects of crystal structure and some crystal chemical applications. *J. Appl. Crystallogr.* **29**, 305-306.

BENTE, K. & KUPČÍK, V. (1984): Redetermination and refinement of the structure of tetrabismuth tetracopper enneasulphide, $Cu_4Bi_4S_9$. *Acta Crystallogr.* **C40**, 1985-1986.

BERLEPSCH, P., MAKOVICKY, E. & BALIĆ-ŽUNIĆ, T. (2001): Crystal chemistry of meneghinite homologues and related sulphosalts. *Neues Jahrb. Mineral., Monatsh.*, 115-135.

BRUKER AXS (1997): SHELXTL, Version 5.1. Bruker AXS, Inc., Madison,Wisconsin 53719,U.S.A.

BRUKER AXS (1998): SMART, Version 5.0. Bruker AXS, Inc., Madison, Wisconsin 53719,U.S.A.

BRUKER AXS (1998): SAINT, Version 5.0. Bruker AXS, Inc., Madison,Wisconsin 53719, U.S.A.

CIOBANU, C.L. & COOK, N.J. (2002): Comparison of primary bismuth associations in two Southern African pegmatites. *Eleventh Quadrennial IAGOD Symposium and Geocongress* (*Windhoek*), *Extended Abstr., Geol. Surv. Namibia*.

CIOFLICA, G. & VLAD, S. (1973): Aikinite in skarn deposits from Baita Bihorului. *Stud. ºi Cerc. Geol., Geofiz., Geogr., Ser. Geol.* **18**, 311-316 (in Romanian).

DANA, E.S. (1892): The System of Mineralogy of James Dwight Dana, 1837–1868 (6th ed.). John Wiley and Sons, Inc., New York, N.Y. (1, 134).

FERRARIS, G., MAKOVICKY, E. & MERLINO, S. (2004): *Crystallography of Modular Materials*. Oxford University Press, Oxford, U.K. (in press).

HILLEBRAND, W.F. (1884): On an interesting variety of löllingite and other minerals. *Am. J. Sci.* **27**, 349-358.

KODĚRA, M., KUPČÍK, V. & MAKOVICKY, E. (1970): Hodrushite – a new sulphosalt. *Mineral. Mag.* **37**, 641-648.

KUPČÍK, V. & MAKOVICKY, E. (1968): Die Kristallstruktur des Minerals (Pb, Ag, Bi)$Cu_4Bi_5S_{11}$. *Neues Jahrb. Mineral., Monatsh.*, 236-239.

MAKOVICKY, E. (1989): Modular classification of sulphosalts – current status. Definition and application of homologous series. *Neues Jahrb. Mineral., Abh.* **160**, 269-297.

_____ (1997): Chapters 3 and 5 *In* Modular Aspects of Minerals (S. Merlino, ed.). *Eur. Mineral. Union, Notes in Mineralogy* **1**, 237-271.

_____ & BALIĆ-ŽUNIĆ, T. (1998): New measure of distortion for coordination polyhedra. *Acta Crystallogr.* **B54**, 766-773.

_____ & KARUP-MØLLER, S. (1977): Chemistry and crystallography of the lillianite homologous series. I. General properties and definitions. *Neues Jahrb. Mineral., Abh.* **130**, 264-287.

_____ & MACLEAN, W.H. (1972): Electron microprobe analysis of hodrushite. *Can. Mineral.* **11**, 504-513.

_____, SØTOFTE, I., & KARUP-MØLLER, S. (2002): The crystal structure of $Cu_4Bi_4Se_9$. *Z. Kristallogr.* **217**, 597-604.

MARIOLACOS, K., KUPČÍK, V., OHMASA, M. & MIEHE, G. (1975): The crystal structure of $Cu_4Bi_5S_{10}$ and its relation to the structures of hodrushite and cuprobismutite. *Acta Crystallogr.* **B31**, 703-708.

MUMME, W.G. (1986): The crystal structure of paderaite, a mineral of the cuprobismutite series. *Can. Mineral*. **24**, 513-521.

NUFFIELD, E.W. (1952): Studies of mineral sulpho-salts. XVI. Cuprobismutite. *Am. Mineral*. **37**, 447-452.

OZAWA, T. & NOWACKI, W. (1975): The crystal structure of, and the bismuth–copper distribution in synthetic cuprobismutite. *Z. Kristallogr*. **142**, 161-176.

SHELDRICK, G.M. (1997a): *SHELXS–97. A Computer Program for Crystal Structure Determination*. University of Göttingen, Göttingen, Germany.

_____ (1997b): *SHELXL–97. A Computer Program for Crystal Structure Refinement*. University of Göttingen, Göttingen, Germany.

SUGAKI, A., KITAKAZE, A. & HAYASHI, T. (1981): Synthesis of minerals in the Cu–Fe–Bi–S system under hydrothermal condition and their phase relations. *Bull. Minéral.* **104**, 484-495.

TAKÉUCHI, Y. & OZAWA, T. (1975): The structure of $Cu_4Bi_4S_9$ and its relation to the structures of covellite, CuS and bismuthinite, Bi_2S_3. *Z. Kristallogr.* **141**, 217-232.

TOPA , D. (2001): *Mineralogy, Crystal Structure and Crystal Chemistry of the Bismuthinite–Aikinite Series from Felbertal, Austria.* Ph.D. thesis, Institute of Mineralogy, University of Salzburg, Austria.

_____, MAKOVICKY, E., BALIĆ-ŽUNIĆ, T. & PAAR, W.H. (2003): Kupčíkite, $Cu_{3.4}Fe_{0.6}Bi_5S_{10}$, a new Cu–Bi sulfosalt from Felbertal, Austria, and its crystal struture. *Can. Mineral.* **41**, 1155-1166.

_____, _____ & PAAR, W.H. (2002): Compositional ranges and exsolution pairs for the members of the bismuthinite–aikinite series from Felbertal, Austria. *Can. Mineral.* **40**, 849-869.

TRÖMEL, M. (1981): Abstandskorrelationen bei der Tellur(IV)-Sauerstoff- und bei der Antimon (III)-Sauerstoff-Koordination. *Z. Kristallogr*. **154,** 338-339.

ŽÁK, L., FRYDA, J., MUMME, W.G. & PAAR, W.H. (1994): Makovickyite, $Ag_{1.5}Bi_{5.5}S_9$ from Băiţa Bihorului, Romania. The ^{4}P natural member of the pavonite series. *Neues Jahrb. Mineral., Abh.* **168**, 147-169.

Received May 8, 2003, revised manuscript accepted November 30, 2003.

APPENDIX

The parameters used for the description of coordination polyhedra were defined by Balić-Žunić & Makovicky (1996) and Makovicky & Balić-Žunić (1998). In the first stage of the procedure, a circumscribed sphere is fitted to all the ligands of the central atom by a least-squares procedure. Sphere radius r_s and sphere volume V_s are typical for the chemical elements involved and the coordination number (CN). The standard deviation σ_r of the radius is used to define "linear sphericity" $SPH_L = (1 - \sigma_r/r)$, or "volume-based sphericity" $SPH_v = (1 - 3\sigma_r/r)$, the latter derived by the error-propagation formula from the formula for the volume of a sphere. Sphericity is a measure of "goodness-of-fit" of the polyhedra observed to the sphere.

Eccentricity describes the displacement of the central atom from the ideal center of the circumscribed sphere, the "centroid". The centroid – central atom distance Δ is used either to define a "linear eccentricity" $ECC_L = \Delta/r$ or a "volume-based eccentricity" $ECC_v = 1 - [(r_s - \Delta)/r_s]^3$. The latter was obtained by comparison of the volumes of the spheres with a radius equal to r_s and $(r_s - \Delta)$, respectively.

A measure of the volume-based distortion is calculated as follows: $\nu = (V_i - V_p)/V_i$, where V_p is the volume of the polyhedron observed, and V_i is the volume of such polyhedron with the ideal shape, both *with the same circumscribed sphere*. The volume of the polyhedron V_p is calculated from the structure, together with V_s, whereas the formula of V_i for the observed CN can be looked up in Makovicky & Balić-Žunić (1998); V_i is then calculated for the given value of r_s. Another expression of this polyhedron distortion is the position of the polyhedron in the V_p *versus* V_s plot: for the given CN, distorted polyhedra have lower values of V_p than the ideal ones (= V_i).

The scatter of the ligands about the least-squares-fitted circumscribed sphere (resulting in the value of σ_r) is a function of the shape of the coordination polyhedron. It is not identical to the uncertainty in the value of the sphere radius or of the calculated sphere or polyhedron volume, because of standard errors of the atom positions.

As demonstrated by Trömel (1981) and illustrated in detail for sulfosalts by Berlepsch *et al.* (2001), in the coordination polyhedra of lone-pair cations, the opposing bonds (or cation–ligand distances) follow a hyperbolic correlation trend, specific for a given element. Besides explaining details of coordination, this analysis allows one to recognize cation disorder and substitution at individual sites.

The notion of archetype and homologous series is useful for compact structures with larger volumes (rods, slabs, blocks) of fairly uniform coordination polyhedra sharing vertices, edges and, in some cases, faces. A homologous series is a series of compounds with structures built of the same type of building blocks (in most cases slabs) cut out along the same planes (*hkl*) of a given archetypal structure. These blocks are joined together by action of structure-building operations, such as unit-cell twinning on mirror or glide planes, crystallographic shear or intergrowths on a unit-cell scale. Members of the series differ in the size of these blocks; the blocks grow incrementally by addition of new layers of coordination polyhedra. The order *N* of a homologue is determined by the number of polyhedra across a suitable diameter of the building block. Each homologue has its own unit cell, chemical composition and structure although all of these follow the same incremental general principles. More detailed definitions, and the relation to a polysomatic description, are given in Makovicky (1989, 1997) and Ferraris *et al.* (2004).